Dirac open-quantum-system dynamics: Formulations and simulations

Renan Cabrera,* Andre G. Campos, Denys I. Bondar, and Herschel A. Rabitz
Department of Chemistry, Princeton University, Princeton, New Jersey 08544, USA
(Received 18 July 2016; published 14 November 2016)

We present an open-system interaction formalism for the Dirac equation. Overcoming a complexity bottleneck of alternative formulations, our framework enables efficient numerical simulations (utilizing a typical desktop) of relativistic dynamics within the von Neumann density matrix and Wigner phase-space descriptions. Employing these instruments, we gain important insights into the effect of quantum dephasing for relativistic systems in many branches of physics. In particular, the conditions for robustness of Majorana spinors against dephasing are established. Using the Klein paradox and tunneling as examples, we show that quantum dephasing does not suppress negative energy particle generation. Hence, the Klein dynamics is also robust to dephasing.

DOI: 10.1103/PhysRevA.94.052111

I. INTRODUCTION

The Dirac equation is a cornerstone of relativistic quantum mechanics [1]. It was originally developed to describe spin-$\frac{1}{2}$ charged particles playing an essential role in the field of high-energy physics [2–4]. Recently, there is resurging interest in the Dirac equation because it was found to be an effective dynamical model of unexpectedly diverse phenomena occurring in high-intensity lasers [5], solid state [6–9], optics [10,11], cold atoms [12,13], trapped ions [14,15], circuit QED [16], and the chemistry of heavy elements [17,18]. However, there is a need to go beyond coherent dynamics offered by the Dirac equation alone in order to model the effects of imperfections, noise, and interaction with a thermal bath [19]. To construct such models, we will first review how these effects are described without relativistic considerations [20].

In the nonrelativistic regime, the Schrödinger equation describes a quantum system isolated from the rest of the universe. This is a good approximation for certain conditions. For example, an atom in a dilute gas can be considered to be a closed system if the time scale of the dynamics is much faster than the mean collision time. If we would like to include collisions in the picture, we need to keep track of the quantum phases of each atom in the gas. This is unfeasible. This type of dynamics motivated development of the theory of *open quantum systems* [21], where a single-particle picture is retained albeit with more general dynamical equations. There are two methods to introduce interactions with an environment: (i) the Schrödinger equation with an additional stochastic force, or (ii) the conceptually different density matrix formalism [20]. In the latter, a state of an open quantum system is represented by a self-adjoint density operator $\hat{\rho}$ with non-negative eigenvalues summing up to one. The master equation, governing evolution of $\hat{\rho}$, reads as

$$i\hbar\frac{d}{dt}\hat{\rho} = [\hat{H},\hat{\rho}] + \mathcal{D}(\hat{\rho}), \tag{1}$$

where $\hat{H}$ is the quantum Hamiltonian and the dissipator $\mathcal{D}(\hat{\rho})$ encodes the interaction with an environment. The von Neumann equation [20] describing unitary evolution is recovered by ignoring the dissipator. When $\mathcal{D}(\hat{\rho}) \neq 0$, Eq. (1) generally does not preserve the von Neumann entropy $S = -\mathrm{Tr}\,(\hat{\rho}\log\hat{\rho})$, which measures the amount of information stored in a quantum system. We note that effective elimination of $\mathcal{D}(\hat{\rho})$ is a fundamental challenge in order to develop many quantum technologies [22,23].

The nonrelativistic theory of open quantum systems provided profound insights into some fundamental questions of physics such as the emergence of the classical world from the quantum one [24–31], measurement theory [24,32–34], quantum chaos [27,30,31,35], and synchrotron radiation [36–38].

To study the quantum-to-classical transition, it is instrumental to put both mechanics on the same mathematical footing [24,25,28,32,39–46]. This is achieved by the Wigner quasiprobability distribution $W(x,p)$ [47], which is a phase-space representation of the density operator $\hat{\rho}$. Note that the Wigner function serves as a basis for a self-consistent phase-space representation of quantum mechanics [43,48], which is equivalent to the density matrix formalism.

Previous attempts to construct the relativistic theory of open quantum system relied on the relativistic extension of the Wigner function without introducing the corresponding density matrix formalism. In Sec. II, we will first present the manifestly covariant density matrix formalism for a Dirac particle and then construct the Wigner representation. The development of the relativistic Wigner function was motivated by applications in quantum plasma dynamics and relativistic statistical mechanics [3]. The manifestly covariant relativistic Wigner formalism for the Dirac equation was put forth in Refs. [2,49–51] (see Ref. [3] for a comprehensive review). In addition, exact solutions for physically relevant systems were reported in Refs. [52,53]. In addition to the formulation of the Wigner function for spin-$\frac{1}{2}$ particles described by the Dirac equation, there are analogous developments for spinless particles [54–56]. The following conceptual difference between the nonrelativistic and relativistic Wigner functions (spin-$\frac{1}{2}$ particles in the relativistic case) was elucidated in Ref. [57]: In nonrelativistic dynamics, Hudson's theorem states that the Wigner function for a pure state is positive if and only if the underlying wave function is a Gaussian [58]. In other cases, the Wigner function contains negative values. However, this statement does not carry over to the relativistic regime. In particular, there are many physically meaningful spinors whose Wigner function is positive [57]. Note that the Wigner

*rcabrera@princeton.edu

 ©2016 American Physical Society

function's negativity is an important resource in quantum information theory [59,60].

The limit $\hbar \to 0$ of the generator of motion for the nonrelativistic Wigner function is nonsingular and recovers classical dynamics. (Note that the classical limit $\hbar \to 0$ of quantum states is a subtle issue that may involve quantum chaos and open-system interactions [31].) The same limiting property is expected from the relativistic extension. However, the manifest covariance of the equations of motion of the relativistic Wigner function needed to be broken in order to perform the $\hbar \to 0$ limit [51,61–64]. From a different perspective, the covariant classical limit was obtained in Refs. [42,65]. In Appendix B of this work, we provide a simpler manifestly covariant derivation of the classical limit. Contrary to the previous work, our derivation recovers two decoupled classical equations of motion: one governing the dynamics of positive energy particles and the other describing negative energy particles (i.e., antiparticles). An alternative quantum field theoretic formulation of the Wigner function for Dirac fermions has also been put forth [61,66–71].

As mentioned before, the current interest in the Dirac equation goes far beyond relativistic physics. These new opportunities come along with new challenges. It is the aim of this article to overcome some of those problems by furnishing a new formulation of traditional (i.e., closed system) relativistic dynamics enabling efficient numerical simulations as well as physically consistent inclusion of open-system interactions. We believe that the developed formalism and numerical methods will influence the following fields:

(1) *Understanding the role of the environment for the classical world emergence.* In particular, we elucidate the influence of decoherence (i.e., loss of quantum phase coherence) on relativistic dynamics in Secs. VI and VII, where Klein tunneling [7] and the associated paradox are analyzed along with the Majorana fermion dynamics.

(2) *Development of the quantum relativistic theory of energy dissipation.* Based on existing models of nonrelativistic quantum friction [72,73], we expect a relativistic model of energy damping to obey (i) the mass-shell constraint, (ii) translational invariance (in particular, the dynamics should not depend on the choice of the origin), (iii) equilibration (the model should reach a steady state at long time propagation; in particular, the final energy at $t \to +\infty$ should be bounded, thereby preventing runaway population of the negative energy continuum), (iv) thermalization (i.e., the achieved steady state should represent thermal equilibrium), (v) relativistic extension of Ehrenfest theorems (i.e., see the dynamical constraints for expectation values encompassing energy drain in Ref. [73]). Some preliminary steps towards the desired relativistic model are reported in Ref. [74].

(3) *Modeling environmental effects in Dirac materials* such as topological insulators [8,75,76], Weyl semimetals [77,78], and graphene [6]. In these cases, open-system dynamics models sample impurities and imperfections as well as external noise. Recently, the Dirac equation with an additional stochastic force was utilized for this purpose [19]. To the best of our knowledge, a more general master-equation formalism is yet to be explored.

(4) *Understanding robustness of a Majorana particle*, which is defined as being its own antiparticle. Experimental implementation of solid-state analogs of Majorana fermions [79–81] opens up possibilities to study the physics of these unusual states. In particular, Majorana bound states are well-suited components of topological quantum computers [82]. Due to its topological nature, Majorana states are expected to be robust against perturbations and imperfections [83]. Dissipative dynamics modeled within a Lindblad master equation confirmed a significant degree of robustness in a specific optical lattice [84]. However, the robustness is not universal [85] and there is a need for enhancement (e.g., employing error-correction techniques [86]). Note that Majorana states studied in condensed matter physics [79–81] do not strictly coincide with the authentic Majorana spinors [87], albeit sharing common features. In this paper, we consider original Dirac Majorana spinors [87]. In Sec. VI, we demonstrate that a single-particle Majorana spinor exhibits robustness even for strong couplings to the dephasing environment, which otherwise quickly washes out interferences for particle-particle superpositions (that is, Schrödinger cat states). Moreover, this phenomenon has an intuitive explanation in the phase-space representation, where quantum dephasing turned out to be equivalent to Gaussian filtering over the momentum axis (detailed explanation in Secs. IV and V). The applicability of this insight to condensed matter systems should be a subject of further studies.

(5) *Development of manifestly covariant quantum-open-system interaction.* Coupling a Dirac particle to the environment generally introduces a preferred frame of reference, thereby breaking the Lorentz invariance. However, coupling to the vacuum, causing spontaneous emission, Lamb shift, etc. [88], and radiation reaction [89,90], needs to be manifestly covariant because the vacuum has no preferred frame of reference. Solid state physics holds a promise to implement many exotic quantum effects experimentally not yet verified [91], e.g., the Unruh effect and Hawking radiation. Solid state dynamics naturally includes the interaction with the environment, thus the need to include open-system interaction into the dynamics of interest. A relativistic quantum theory of measurements also requires development of manifestly covariant master equations. Currently, approaches based on axiomatics [92] and stochastic Dirac and Lindblad master equations [93] are explored. Nevertheless, the proposed equations are computationally unfeasible at present. In this work, we lay the ground for a computationally efficient technique by introducing a manifestly covariant von Neumann equation (see Sec. II) based on Refs. [2,3,49–51].

This paper is organized in seven sections and two appendixes. Section II provides the general mathematical formalism including the manifestly relativistic covariant von Neumann equation. Section III is concerned with the relativistic Wigner function and related representations. Section IV introduces open-system interactions by considering a model of dephasing, environmental interaction leading to the loss of quantum phase. Numerical algorithms are developed in Sec. V and illustrated for the dynamics of Majorana spinors and the Klein paradox in Secs. VI and VII, respectively. The final section VIII provides the conclusions. Appendix A treats the concept of relativistic covariance, and Appendix B elaborates the classical limit ($\hbar \to 0$) of the Dirac equation in manifestly covariant fashion.

II. GENERAL FORMALISM

Note that throughout the paper, $\boldsymbol{x}$ and x denote different variables; likewise, $\hat{\boldsymbol{x}}$ and $\hat{x}$ denote different operators. In addition, Greek characters (e.g., μ, ν), used as indices for Minkowski vectors, are assumed to run from 0 to 3, while, Latin indices (e.g., j,k) run from 1 to 3. The Minkowski metric is a diagonal matrix diag$(1,-1,-1,-1)$. This implies that $x^0 = x_0$ and $x^k = -x_k$.

The manifestly covariant Dirac equation reads as

$$D(\hat{\boldsymbol{x}}^\mu, \hat{\boldsymbol{p}}_\mu)|\psi\rangle = 0, \tag{2}$$

where the Dirac generator $D(\hat{\boldsymbol{x}}^\mu, \hat{\boldsymbol{p}}_\mu)$ and the commutation relations are defined as

$$D(\hat{\boldsymbol{x}}^\mu, \hat{\boldsymbol{p}}_\mu) = \gamma^\mu[c\hat{\boldsymbol{p}}_\mu - eA_\mu(\hat{\boldsymbol{x}})] - mc^2, \tag{3}$$

$$[\hat{\boldsymbol{x}}^\mu, \hat{\boldsymbol{p}}_\nu] = -i\hbar\delta^\mu{}_\nu. \tag{4}$$

Note that the negative sign in the right-hand side of Eq. (4) occurs due to the fact

$$[\hat{\boldsymbol{x}}^k, \hat{\boldsymbol{p}}_j] = -i\hbar\delta^k{}_j \longleftrightarrow [\hat{\boldsymbol{x}}^k, \hat{\boldsymbol{p}}^j] = i\hbar\delta^{kj}, \tag{5}$$

in agreement with nonrelativistic dynamics where the momentum is expressed in contravariant components $\hat{\boldsymbol{p}}^j$.

From the well-established work on relativistic statistical quantum mechanics [2,3,49–51], the manifestly covariant von Neumann equation can be written as

$$D(\hat{\boldsymbol{x}}^\mu, \hat{\boldsymbol{p}}^\mu)\hat{P} = 0, \quad \hat{P}D(\hat{\boldsymbol{x}}^\mu, \hat{\boldsymbol{p}}^\mu) = 0, \tag{6}$$

where $\hat{P}$ represents the density state operator acting on the *manifestly covariant spinorial Hilbert space* (MCS). Equation (6) is the foundation for all the subsequent developments.

Following Refs. [94,95], we introduce the *manifestly covariant Hilbert phase space* (MCP) where the algebra of observables consists of $(\hat{\boldsymbol{x}}, \hat{\boldsymbol{p}}_\mu)$ [see Eq. (4)] along with the mirror operators $(\hat{\boldsymbol{x}}'^\mu, \hat{\boldsymbol{p}}'_\mu)$ obeying

$$[\hat{\boldsymbol{x}}^\mu, \hat{\boldsymbol{p}}_\nu] = -i\hbar\delta^\mu{}_\nu, \quad [\hat{\boldsymbol{x}}'^\mu, \hat{\boldsymbol{p}}'_\nu] = i\hbar\delta^\mu{}_\nu, \tag{7}$$

and all the other commutators vanish. In MCP the role of density operator $\hat{P}$ is taken over by the ket state $|P\rangle$ according to

$$\hat{O}(\hat{\boldsymbol{x}}^\mu, \hat{\boldsymbol{p}}^\mu)\hat{P} \quad \longleftrightarrow \quad \overrightarrow{O}(\hat{\boldsymbol{x}}^\mu, \hat{\boldsymbol{p}}^\mu)|P\rangle, \tag{8}$$

$$\hat{P}\hat{O}(\hat{\boldsymbol{x}}^\mu, \hat{\boldsymbol{p}}^\mu) \quad \longleftrightarrow \quad |P\rangle\overleftarrow{O}(\hat{\boldsymbol{x}}'^\mu, \hat{\boldsymbol{p}}'^\mu), \tag{9}$$

where the arrows indicate the direction of application of the operators $O(\hat{\boldsymbol{x}}^\mu, \hat{\boldsymbol{p}}^\mu)$ and $O(\hat{\boldsymbol{x}}'^\mu, \hat{\boldsymbol{p}}'^\mu)$. Thus, the relativistic von Neumann equation (6) reads in MCP as

$$\overrightarrow{D}(\hat{\boldsymbol{x}}^\mu, \hat{\boldsymbol{p}}^\mu)|P\rangle = 0, \qquad |P\rangle\overleftarrow{D}(\hat{\boldsymbol{x}}'^\mu, \hat{\boldsymbol{p}}'^\mu) = 0. \tag{10}$$

A summary of the two introduced formulations is given in Table I.

The manifest covariance of Eq. (10) can be relaxed to implicit covariance by separating the time according to the $3+1$ splitting $\hat{\boldsymbol{x}}^\mu = (c\hat{\boldsymbol{t}}, \hat{\boldsymbol{x}}^k)$ [96]. This means that the underlying relativistic covariance is maintained but it is no longer evident. In the spirit of the $3+1$ scheme, we define the

TABLE I. Two manifestly covariant formulations of relativistic quantum mechanics.

	Manifestly covariant spinorial Hilbert space (MCS)	Manifestly covariant Hilbert phase space (MCP)
State	$\hat{P}$	$\lvert P\rangle$
Operators	$\hat{O}(\hat{\boldsymbol{x}}^\mu, \hat{\boldsymbol{p}}^\mu)$	$\overrightarrow{O}(\hat{\boldsymbol{x}}^\mu, \hat{\boldsymbol{p}}^\mu)$, $\overleftarrow{O}(\hat{\boldsymbol{x}}'^\mu, \hat{\boldsymbol{p}}'^\mu)$
Equation of motion	$D(\hat{\boldsymbol{x}}^\mu, \hat{\boldsymbol{p}}^\mu)\hat{P} = 0$	$\overrightarrow{D}(\hat{\boldsymbol{x}}^\mu, \hat{\boldsymbol{p}}^\mu)\lvert P\rangle = 0$
	$\hat{P}D(\hat{\boldsymbol{x}}^\mu, \hat{\boldsymbol{p}}^\mu) = 0$	$\lvert P\rangle\overleftarrow{D}(\hat{\boldsymbol{x}}'^\mu, \hat{\boldsymbol{p}}'^\mu) = 0$

Dirac Hamiltonian as

$$\hat{H} = \alpha^k[c\hat{\boldsymbol{p}}^k - eA^k(\hat{\boldsymbol{t}}, \hat{\boldsymbol{x}}^k)] + mc^2\gamma^0 + eA^0(\hat{\boldsymbol{t}}, \hat{\boldsymbol{x}}^k). \tag{11}$$

The von Neumann equation (10) in the *implicit covariant Hilbert phase space* (ICP) becomes

$$[c\overrightarrow{\hat{\boldsymbol{p}}_0} - \overrightarrow{H}(\hat{\boldsymbol{t}}, \hat{\boldsymbol{x}}^k, \hat{\boldsymbol{p}}_k)]|P\rangle\gamma^0 = 0, \tag{12}$$

$$|P\rangle\gamma^0[c\overleftarrow{\hat{\boldsymbol{p}}'_0} - \overleftarrow{H}(\hat{\boldsymbol{t}}', \hat{\boldsymbol{x}}'^k, \hat{\boldsymbol{p}}'_k)] = 0. \tag{13}$$

Inspired by the Bopp transformations in the nonrelativistic quantum mechanical phase space [97,98], a representation of the algebra (7) can be constructed in terms of ICP Bopp operators $(\hat{t}, \hat{\tau}, \hat{\Omega}, \hat{E}, \hat{x}^k, \hat{p}_k, \hat{\lambda}_k, \hat{\theta}^k)$ in Table II, obeying

$$[\hat{t}, \hat{E}] = -i\hbar, \quad [\hat{\Omega}, \hat{\tau}] = -i\hbar, \tag{14}$$

$$[\hat{x}^j, \hat{\lambda}_k] = -i\delta^j{}_k, \quad [\hat{p}_j, \hat{\theta}^k] = -i\delta^k{}_j, \tag{15}$$

where all the other commutators vanish, in particular $[\hat{x}^k, \hat{p}_j] = 0$. A graphical illustration of the relation between the time variables $\boldsymbol{t}$-$\boldsymbol{t}'$ and t-τ is shown in Fig. 1. Adding and subtracting Eqs. (12) and (13), and utilizing the Bopp operators, we obtain the von Neumann equation in the ICP space

$$\hat{E}|P\rangle\gamma^0 = \overrightarrow{H}\left(\hat{t} - \frac{\hat{\tau}}{2}, \hat{x}^k - \frac{\hbar}{2}\hat{\theta}^k, \hat{p}_k + \frac{\hbar}{2}\hat{\lambda}_k\right)|P\rangle\gamma^0 - |P\rangle\gamma^0\overleftarrow{H}\left(\hat{t} + \frac{\hat{\tau}}{2}, \hat{x}^k + \frac{\hbar}{2}\hat{\theta}^k, \hat{p}_k - \frac{\hbar}{2}\hat{\lambda}_k\right), \tag{16}$$

$$2c\hat{\Omega}|P\rangle\gamma^0 = \overrightarrow{H}\left(\hat{t} - \frac{\hat{\tau}}{2}, \hat{x}^k - \frac{\hbar}{2}\hat{\theta}^k, \hat{p}_k + \frac{\hbar}{2}\hat{\lambda}_k\right)|P\rangle\gamma^0 + |P\rangle\gamma^0\overleftarrow{H}\left(\hat{t} + \frac{\hat{\tau}}{2}, \hat{x}^k + \frac{\hbar}{2}\hat{\theta}^k, \hat{p}_k - \frac{\hbar}{2}\hat{\lambda}_k\right). \tag{17}$$

TABLE II. Operators in the *implicitly covariant Hilbert phase* space (ICP) where $(\hat{t}, \hat{\tau}, \hat{\Omega}, \hat{E}, \hat{x}^k, \hat{p}_k, \hat{\lambda}_k, \hat{\theta}^k)$ represent the ICP Bopp operators.

	ICP operators	Mirror ICP operators
Space-time	$\hat{\boldsymbol{t}} = \hat{t} - \frac{1}{2}\hat{\tau}$	$\hat{\boldsymbol{t}}' = \hat{t} + \frac{1}{2}\hat{\tau}$
	$\hat{\boldsymbol{x}}^k = \hat{x}^k - \frac{\hbar}{2}\hat{\theta}^k$	$\hat{\boldsymbol{x}}'^k = \hat{x}^k + \frac{\hbar}{2}\hat{\theta}^k$
Momentum energy	$\hat{\boldsymbol{p}}_0 = \hat{\Omega} + \frac{1}{2c}\hat{E}$	$\hat{\boldsymbol{p}}'_0 = \hat{\Omega} - \frac{1}{2c}\hat{E}$
	$\hat{\boldsymbol{p}}_k = \hat{p}_k + \frac{\hbar}{2}\hat{\lambda}_k$	$\hat{\boldsymbol{p}}'_k = \hat{p}_k - \frac{\hbar}{2}\hat{\lambda}_k$

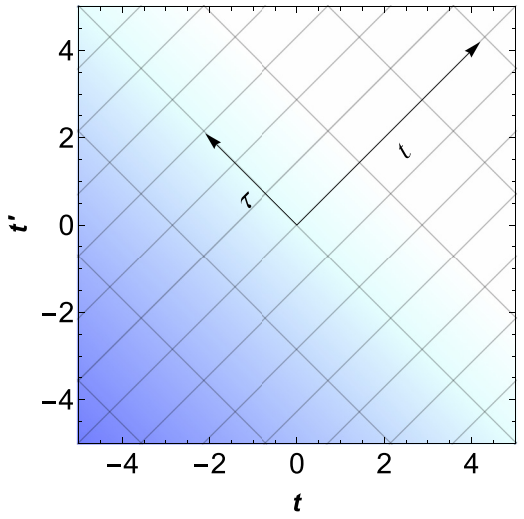

FIG. 1. Graphical illustration of the relation between the double time variables in the ICP space as defined in Table II. The color gradient is directed along the t coordinate.

$\hat{E}$ and $\hat{\Omega}$ can be realized in terms of differential operators as

$$\hat{t} = t, \quad \hat{E} = i\hbar\frac{\partial}{\partial t}, \tag{18}$$

$$\hat{\tau} = \tau, \quad \hat{\Omega} = i\hbar\frac{\partial}{\partial \tau}, \tag{19}$$

turning Eqs. (16) and (17) into a system of two differential equations that can be solved by either propagating along t while keeping τ fixed, or moving along τ with t constant. In particular, setting $\tau = 0$ in Eq. (16), we obtain the relativistic von Neumann equation in the *sliced covariant Hilbert phase space* (SCP)

$$i\hbar\frac{d}{dt}|P\rangle\gamma^0 = \overrightarrow{H}\left(\hat{t},\hat{x}^k - \frac{\hbar}{2}\hat{\theta}^k, \hat{p}_k + \frac{\hbar}{2}\hat{\lambda}_k\right)|P\rangle\gamma^0 - |P\rangle\gamma^0\overleftarrow{H}\left(\hat{t},\hat{x}^k + \frac{\hbar}{2}\hat{\theta}^k, \hat{p}_k - \frac{\hbar}{2}\hat{\lambda}_k\right). \tag{20}$$

It is well known that a Lorentz transformation mixes the space and time degrees of freedom, as recapitulated in Appendix A. In particular, the time evolution of the state in a different reference frame corresponds to a different slicing in the t-τ plane. Therefore, the state propagated by Eq. (20) with $\tau = 0$ does not contain enough information to deduce the observations from a different inertial frame of reference. Nevertheless, Eq. (20) represents a consistent relativistic equation of motion describing dynamics from the particular frame of reference (corresponding to the $\tau = 0$ slice) free of any nonphysical artifacts, e.g., superluminal propagation. A schematic illustration of slicing dynamics at $\tau = 0$ is shown in Fig. 2. Note that equations of motion containing two time variables also appear in nonrelativistic dynamics [99].

Using Table II, we rewrite Eq. (20) in the Hilbert spinorial space

$$i\hbar\frac{d}{dt}\hat{P}\gamma^0 = [H(t,\hat{\boldsymbol{x}}^k,\hat{\boldsymbol{p}}_k),\hat{P}\gamma^0]. \tag{21}$$

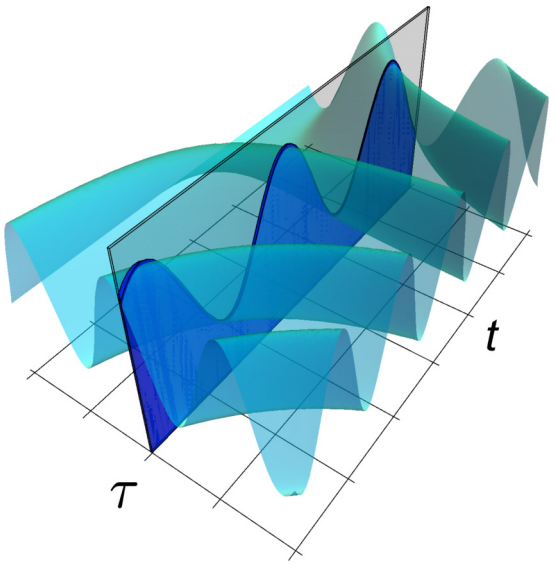

FIG. 2. Schematic illustration of a quantum state propagating along time t within the slice $\tau = 0$ according to Eq. (20). A different inertial reference frame would generate another slice.

Note that this equation resembles Eq. (1) with $\mathcal{D} = 0$. In other words, we obtain a straightforward relativistic extension of the density matrix formalism for the Dirac equation. Migdal [100] employed Eq. (21) to describe the effect of multiple scattering on bremsstrahlung and pair production.

III. RELATIVISTIC WIGNER FUNCTION

This section is devoted to study specific representations of the von Neumann equation in the SCP space (20) in order to derive the time evolution of the relativistic Wigner function.

Following Table II, there are four representations of interest:

(i) The *double configuration space* is defined by setting

$$\hat{x}^k = x^k, \quad \hat{\theta}^k = \theta^k, \quad \hat{\lambda}_k = i\frac{\partial}{\partial x^k}, \quad \hat{p}_k = -i\frac{\partial}{\partial \theta^k}. \tag{22}$$

Hence, the equation of motion (20) becomes

$$i\hbar\frac{\partial B\gamma^0}{\partial t} = \overrightarrow{H}\left(t,x^k - \frac{\hbar}{2}\theta^k, \hat{p}_k + \frac{\hbar}{2}\hat{\lambda}_k\right)B\gamma^0 - B\gamma^0\overleftarrow{H}\left(t,x^k + \frac{\hbar}{2}\theta^k, \hat{p}_k - \frac{\hbar}{2}\hat{\lambda}_k\right), \tag{23}$$

where B is defined as the relativistic Blokhintsev function

$$B\gamma^0 = \frac{1}{\sqrt{\hbar}}\langle x^k,\theta^k|P\rangle\gamma^0 = \left\langle x^k - \frac{\hbar}{2}\theta^k\middle|\hat{P}\gamma^0\middle|x^k + \frac{\hbar}{2}\theta^k\right\rangle. \tag{24}$$

For pure states, B is expressed in terms of the four-column Dirac spinor ψ as

$$B(t,x^k,\theta^k)\gamma^0 = \psi\left(t,x^k - \frac{\hbar}{2}\theta^k\right)\psi^\dagger\left(t,x^k + \frac{\hbar}{2}\theta^k\right). \tag{25}$$

Therefore, B is a 4×4 complex matrix-valued function of two degrees of freedom $x - \theta$. The nonrelativistic version of the Blokhintsev function was introduced in Refs. [101–103].

(ii) The *phase space* is defined by

$$\hat{x}^k = x^k, \quad \hat{p}_k = p_k, \quad \hat{\lambda}_k = i\frac{\partial}{\partial x^k}, \quad \hat{\theta}^k = i\frac{\partial}{\partial p_k}. \tag{26}$$

The underlying equation of motion (20) reads as

$$i\hbar\frac{\partial W\gamma^0}{\partial t} = \overrightarrow{H}\left(t, x^k - \frac{\hbar}{2}\hat{\theta}^k, p_k + \frac{\hbar}{2}\hat{\lambda}_k\right)W\gamma^0 - W\gamma^0\overleftarrow{H}\left(t, x^k + \frac{\hbar}{2}\hat{\theta}^k, p_k - \frac{\hbar}{2}\hat{\lambda}_k\right), \tag{27}$$

where W is the sought after relativistic Wigner function

$$W\gamma^0 = \frac{1}{2\pi\hbar}\langle x^k, p^k|P\rangle\gamma^0, \tag{28}$$

which can be recovered from the Blokhintsev function through a Fourier transform

$$W(t, x^k, p^k) = \frac{1}{(2\pi)^3}\int B(t, x^k, \theta^k)\exp(ip\,\theta)d^3\theta. \tag{29}$$

Note that only contravariant components are used in Eqs. (28) and (29).

(iii) The *reciprocal phase space* is defined as

$$\hat{x}^k = -i\frac{\partial}{\partial\lambda_k}, \quad \hat{p}_k = -i\frac{\partial}{\partial\theta^k}, \quad \hat{\lambda}_k = \lambda_k, \quad \hat{\theta}^k = \theta^k. \tag{30}$$

The corresponding equation of motion is

$$i\hbar\frac{\partial\mathcal{A}\gamma^0}{\partial t} = \overrightarrow{H}\left(t, \hat{x}^k - \frac{\hbar}{2}\theta^k, \hat{p}_k + \frac{\hbar}{2}\lambda_k\right)\mathcal{A}\gamma^0 - \mathcal{A}\gamma^0\overleftarrow{H}\left(t, \hat{x}^k + \frac{\hbar}{2}\theta^k, \hat{p}_k - \frac{\hbar}{2}\lambda_k\right), \tag{31}$$

where $\mathcal{A}$ is the relativistic ambiguity function

$$\mathcal{A}\gamma^0 = \frac{1}{\sqrt{\hbar}}\langle\lambda^k, \theta^k|P\rangle\gamma^0, \tag{32}$$

which is recovered from the Blokhintsev function according to

$$A(t, \lambda^k, \theta^k) = \int B(t, x^k, \theta^k)\exp(-ix\,\lambda)d^3x. \tag{33}$$

(iv) The *double momentum space* (see Fig. 3) is introduced as

$$\hat{x}^k = -i\frac{\partial}{\partial\lambda_k}, \quad \hat{p}_k = p_k, \quad \hat{\lambda}_k = \lambda, \quad \hat{\theta}^k = i\frac{\partial}{\partial p_k}. \tag{34}$$

The corresponding equation of motion is

$$i\hbar\frac{\partial Z\gamma^0}{\partial t} = \overrightarrow{H}\left(t, \hat{x}^k - \frac{\hbar}{2}\hat{\theta}^k, p_k + \frac{\hbar}{2}\lambda_k\right)Z\gamma^0 - Z\gamma^0\overleftarrow{H}\left(t, \hat{x}^k + \frac{\hbar}{2}\hat{\theta}^k, p_k - \frac{\hbar}{2}\lambda_k\right), \tag{35}$$

where

$$Z\gamma^0 = \frac{1}{\sqrt{\hbar}}\langle\lambda^k, p^k|P\rangle\gamma^0 = \left\langle p^k + \frac{\hbar}{2}\lambda^k\middle|\hat{P}\gamma^0\middle|p^k - \frac{\hbar}{2}\lambda^k\right\rangle, \tag{36}$$

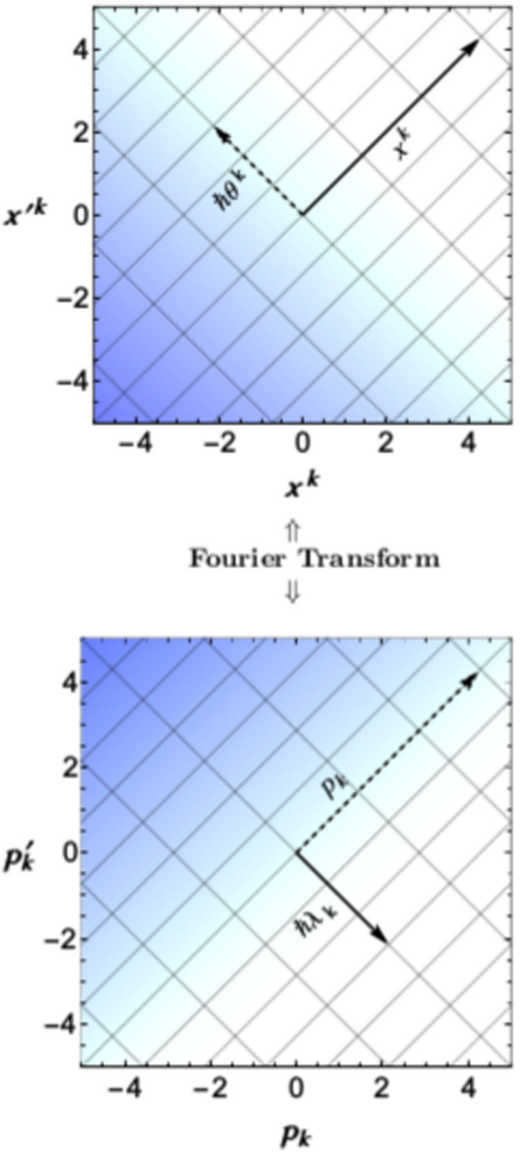

FIG. 3. Relation between the double configuration $(x^k - \theta^k)$ and the double momentum $(\lambda_k - p_k)$ spaces as defined in Table II. The dashed axes along p_k and λ_k indicate that they are related via a direct Fourier transform. The solid axes along x^k and θ^k indicate a similar connection. These relations are also schematically presented in Eq. (39).

which is related with the Wigner function via

$$W(t, x^k, p^k) = \frac{1}{(2\pi)^3}\int Z(t, \lambda^k, p^k)\exp(ix\,\lambda)d^3\lambda. \tag{37}$$

Similarly, we also have

$$\mathcal{A}(t, \lambda^k, \theta^k) = \int Z(t, \lambda^k, p^k)\exp(-ip\,\theta)d^3p. \tag{38}$$

In summary, all these four functions are connected through Fourier transforms as visualized in the following diagram:

$$\begin{array}{ccc} W(x,p) & \xrightarrow{\mathcal{F}_{x\to\lambda}} & Z(\lambda,p) \\ {\scriptstyle \mathcal{F}_{\theta\to p}}\uparrow & & \uparrow{\scriptstyle \mathcal{F}_{\theta\to p}} \\ B(x,\theta) & \xrightarrow{\mathcal{F}_{x\to\lambda}} & \mathcal{A}(\lambda,\theta) \end{array} \tag{39}$$

where vertical arrows denote the direct $\mathcal{F}_{\theta\to p}$ Fourier transforms while horizontal arrows indicate the direct $\mathcal{F}_{x\to\lambda}$ Fourier transforms. A similar diagram can be drawn in terms of the inverse Fourier transforms as

$$\begin{array}{ccc} W(x,p) & \xleftarrow{\mathcal{F}^{\lambda\to x}} & Z(\lambda,p) \\ \downarrow{\scriptstyle \mathcal{F}_{p\to\theta}} & & \downarrow{\scriptstyle \mathcal{F}_{p\to\theta}} \\ B(x,\theta) & \xleftarrow{\mathcal{F}^{\lambda\to x}} & \mathcal{A}(\lambda,\theta) \end{array} \tag{40}$$

Since the relativistic Wigner function W is a 4×4 complex matrix, its visualization is cumbersome. Nevertheless, most of the information is contained in [57]

$$W^0(t,x^k,p^k) \equiv \mathrm{Tr}\,[W(t,x^k,p^k)\gamma^0]/4. \tag{41}$$

In fact, this zeroth component is sufficient to obtain the probability density $j^0 \equiv \psi^\dagger(t,x^k)\psi(t,x^k)$ as

$$\int W^0(t,x^k,p^k)d^3p = \psi^\dagger(t,x^k)\psi(t,x^k), \tag{42}$$

$$\int W^0(t,x^k,p^k)d^3x = \widetilde{\psi}^\dagger(t,p^k)\widetilde{\psi}(t,p^k), \tag{43}$$

where $\widetilde{\psi}$ is the Dirac spinor in the momentum representation, i.e., the Fourier transform of ψ.

Equations (42) and (43) reveal that the zeroth component of the relativistic Wigner function (41) acts as a quasiprobability distribution, a real-valued nonpositive function, whose marginals coincide with the coordinate and momentum probability densities, respectively.

IV. OPEN-SYSTEM INTERACTIONS

Inspired by nonrelativistic quantum mechanics [see Eq. (1)], we add a dissipator to the relativistic von Neumann equation (21) to account for open-system dynamics

$$i\hbar\frac{d}{dt}\hat{P}\gamma^0 = [H(t,\hat{\boldsymbol{x}}^k,\hat{\boldsymbol{p}}^k),\hat{P}\gamma^0] + i\hbar\mathcal{D}(\hat{P}\gamma^0). \tag{44}$$

The operator $\hat{P}\gamma^0$ must remain non-negative at all times in order to represent a physical system. This restricts the form of the dissipator $i\hbar\mathcal{D}(\hat{P}\gamma^0)$. In particular, the Lindblad form

$$i\hbar\mathcal{D}(\hat{P}\gamma^0) = A\hat{P}\gamma^0A^\dagger + \tfrac{1}{2}(A^\dagger A\hat{P}\gamma^0 + \hat{P}\gamma^0A^\dagger A) \tag{45}$$

guarantees the non-negativity. We note that Eq. (44) does not need to comply with relativistic covariance. Nevertheless, this is not a deficiency when dealing with environments such as thermal baths that are typically furnished with a preferred frame of reference.

The following Lindbladian dissipator describes the transversal spreading of a relativistic electron beam undergoing multiple scattering [104] (e.g., bremsstrahlung and pair production in the bulk [100])

$$i\hbar\mathcal{D}[\hat{P}\gamma^0] = -\frac{D}{\hbar^2}[\hat{\boldsymbol{x}}^k,[\hat{\boldsymbol{x}}^k,\hat{P}\gamma^0]], \tag{46}$$

where no summation on k is implied and D shall be referred to as the decoherence coefficient. In the nonrelativistic case, this interaction is utilized to describe the loss of coherence due to the interaction with a high-temperature bath [20,25,29,41,105]. In addition, a system undergoing continuous measurements in position follows the same decoherent dynamics [28,106].

The dynamical effect of an interaction can be characterized by calculating the time derivative of the expectation value of an observable $\hat{O}$:

$$\frac{d}{dt}\langle\hat{O}\rangle = \mathrm{Tr}\left[\frac{d}{dt}(\hat{P}\gamma^0)\hat{O}\right]. \tag{47}$$

Assuming that the equation of motion is of the form

$$\frac{d}{dt}\hat{P}\gamma^0 = \mathcal{M}(\hat{P}\gamma^0), \tag{48}$$

the time derivative of $\langle\hat{O}\rangle$ is expressed as follows:

$$\frac{d}{dt}\langle\hat{O}\rangle = \mathrm{Tr}[\mathcal{M}(\hat{P}\gamma^0)\hat{O}] = \mathrm{Tr}[\hat{P}\gamma^0\mathcal{M}^\dagger(\hat{O})], \tag{49}$$

where $\mathcal{M}^\dagger$ is the adjoint operator of $\mathcal{M}$ with respect to the Hilbert-Schmidt scalar product.

The particular dephasing dissipator (46) is self-adjoint,

$$\mathcal{D}^\dagger[\hat{O}] = \mathcal{D}[\hat{O}]; \tag{50}$$

as a result,

$$\mathcal{D}^\dagger[\hat{\boldsymbol{x}}^k] = \mathcal{D}^\dagger[\hat{\boldsymbol{p}}^k] = 0. \tag{51}$$

This means that the dephasing does not change the Heisenberg equations of motion for position and momentum observables. The open-system interaction affects the dynamics of the second-order momentum

$$\mathcal{D}^\dagger[\hat{\boldsymbol{x}}^k\hat{\boldsymbol{x}}^j] = 0, \quad \mathcal{D}^\dagger[\hat{\boldsymbol{p}}^k\hat{\boldsymbol{p}}^j] = 2D\delta^{kj}, \quad \mathcal{D}^\dagger[\hat{\boldsymbol{x}}^k\hat{\boldsymbol{p}}^j] = 0, \tag{52}$$

which in turn leads to a momentum wave-packet broadening. Moreover, considering that the free Dirac Hamiltonian (11) is linear in momentum, we obtain from Eqs. (51) and (49)

$$\frac{d}{dt}\langle\gamma^0\gamma^k\hat{\boldsymbol{p}}_k + mc\gamma^0\rangle = 0. \tag{53}$$

In other words, the energy is conserved under the action of the dephasing dissipator (46). This is in stark contrast to nonrelativistic dephasing, which is characterized by monotonically increasing energy.

The classical limit of dephasing (46) is diffusion. Relativistic extensions of diffusion face fundamental challenges [107]. For instance, large values of D may induce dynamics leading to superluminal propagation, which breaks down the causality of the Dirac equation (see, e.g., Theorem 1.2 of Ref. [108]). The length scale of diffusion is $\sqrt{\langle x^2\rangle} = \sqrt{2Dt}$; hence, the characteristic speed $\sqrt{\langle x^2\rangle}/t = \sqrt{2D/t}$ must be smaller than the speed of light. The shortest time interval for which the single-particle picture is valid $t \sim \hbar/(2mc^2)$, i.e., the *zitterbewegung* time scale. Considering all these arguments, we obtain

the constraint $D \ll \hbar/(4m)$ or, equivalently, $4D/c \ll \lambda\!\!\!^{-}$ [where $\lambda\!\!\!^{-} = \hbar/(mc)$ is the reduced Compton wavelength] in order to maintain causal dephasing dynamics.

This dephasing interaction (46) can be expressed in the SCP space, leading to a very simple expression [95]

$$\frac{\partial}{\partial t}\langle x^j\theta^j|P\rangle = -D\,\theta^k\theta^k\delta^{kj}\langle x^j\theta^j|P\rangle, \tag{54}$$

which is convenient for numerical propagation, as shown in Sec. V.

V. NUMERICAL ALGORITHM

Stimulated by the resurgent interest in the Dirac equation, a plethora of propagation methods were recently developed [109–114]. However, to the best our knowledge Ref. [115] is the only work devoted to propagation of the relativistic von Neumann equation (21), albeit without open-system interactions. The purpose of this section is to develop an effective numerical algorithm to propagate the master equation (44) describing quantum dephasing (46). The computational effort with the proposed algorithm scales as the square of the Dirac equation propagation complexity. This algorithmic development enables the relativistic Wigner function simulations, which were previously hindered by the complexity of the underlying integrodifferential equations [49,51].

The evolution governed by Eq. (21),

$$i\hbar\frac{d}{dt}\hat{Q} = [H(t,\boldsymbol{x}^k,\hat{\boldsymbol{p}}_k),\hat{Q}], \tag{55}$$

with $\hat{Q} = \hat{P}\gamma^0$, is equivalent to

$$\hat{Q}_{t+dt} = e^{-idtH(t,\hat{\boldsymbol{x}},\hat{\boldsymbol{p}})/\hbar}\hat{Q}_t e^{idtH(t,\hat{\boldsymbol{x}},\hat{\boldsymbol{p}})/\hbar}, \tag{56}$$

where dt is an infinitesimal time step.

Considering that the Hamiltonian can be decomposed as

$$\hat{H} = K(\hat{\boldsymbol{p}}) + V(\hat{\boldsymbol{x}}), \tag{57}$$

$$K(\hat{\boldsymbol{p}}) = c\alpha^k\hat{\boldsymbol{p}}^k + mc^2\gamma^0/2, \tag{58}$$

$$V(\hat{\boldsymbol{x}}) = eA^0(t,\hat{\boldsymbol{x}}^k) - e\alpha^k A^k(t,\hat{\boldsymbol{x}}^k) + mc^2\gamma^0/2, \tag{59}$$

where the mass term contributes to both $K(\hat{\boldsymbol{p}})$ and $V(\hat{\boldsymbol{x}})$. The first-order splitting with error $O(dt^2)$ is then

$$\hat{Q}_{t+dt} = e^{-idtV(\hat{\boldsymbol{x}})/\hbar}e^{-idtK(\hat{\boldsymbol{p}})/\hbar}\hat{Q}_t e^{idtK(\hat{\boldsymbol{p}})/\hbar}e^{idtV(\hat{\boldsymbol{x}})/\hbar}, \tag{60}$$

which implies a two-step propagation

$$\hat{Q}^{1/2} = e^{-idtK(\hat{\boldsymbol{p}})/\hbar}\hat{Q}_t e^{idtK(\hat{\boldsymbol{p}})/\hbar}, \tag{61}$$

$$\hat{Q}_{t+dt} = e^{-idtV(\hat{\boldsymbol{x}})/\hbar}\hat{Q}^{1/2}e^{idtV(\hat{\boldsymbol{x}})/\hbar} \tag{62}$$

Using Eqs. (8) and (9), we move to SCP:

$$|Q^{1/2}\rangle = e^{-idt\overrightarrow{K}(\hat{\boldsymbol{p}})/\hbar}|Q_t\rangle e^{idt\overleftarrow{K}(\hat{\boldsymbol{p}}')/\hbar}, \tag{63}$$

$$|Q_{t+dt}\rangle = e^{-idt\overrightarrow{V}(\hat{\boldsymbol{x}})/\hbar}|Q^{1/2}\rangle e^{idt\overleftarrow{V}(\hat{\boldsymbol{x}}')/\hbar}. \tag{64}$$

Note that $|Q_t\rangle$ is a complex 4×4 matrix reflecting the spinor degrees of freedom. The arrows can be eliminated by choosing suitable bases

$$\langle \boldsymbol{p}\boldsymbol{p}'|Q^{1/2}\rangle = e^{-idtK(\hat{\boldsymbol{p}})/\hbar}\langle \boldsymbol{p}\boldsymbol{p}'|Q_t\rangle e^{idtK(\hat{\boldsymbol{p}}')/\hbar}, \tag{65}$$

$$\langle \boldsymbol{x}\boldsymbol{x}'|Q^{1/2}\rangle = \mathcal{F}_{\boldsymbol{p}\boldsymbol{p}'\to\boldsymbol{x}\boldsymbol{x}'}\langle \boldsymbol{p}\boldsymbol{p}'|Q^{1/2}\rangle, \tag{66}$$

$$\langle \boldsymbol{x}\boldsymbol{x}'|Q_{t+dt}\rangle = e^{-idtV(\hat{\boldsymbol{x}})/\hbar}\langle \boldsymbol{x}\boldsymbol{x}'|Q^{1/2}\rangle e^{idtV(\hat{\boldsymbol{x}}')/\hbar}, \tag{67}$$

$$\langle \boldsymbol{p}\boldsymbol{p}'|Q_{t+dt}\rangle = \mathcal{F}^{\boldsymbol{x}\boldsymbol{x}'\to\boldsymbol{p}\boldsymbol{p}'}\langle \boldsymbol{x}\boldsymbol{x}'|Q_{t+dt}\rangle, \tag{68}$$

where $\mathcal{F}_{\boldsymbol{p}\boldsymbol{p}'\to\boldsymbol{x}\boldsymbol{x}'}$ and $\mathcal{F}^{\boldsymbol{x}\boldsymbol{x}'\to\boldsymbol{p}\boldsymbol{p}'}$ stand for Fourier transforms from the momentum representation to the position representation and vice versa. Considering that the state is a 4×4 matrix, the Fourier transform is independently applied to each matrix component. From the computational perspective, the fast Fourier transform is employed. Further details about the phase-space propagation via the fast Fourier transform can be found in Sec. III of Ref. [95].

Having described the propagation algorithm in SCP $(\hat{\boldsymbol{x}}^k,\hat{\boldsymbol{x}}^{k\prime},\hat{\boldsymbol{p}}^k,\hat{\boldsymbol{p}}^{k\prime})$, one can apply a similar strategy to the Bopp operators $(\hat{x}^k,\hat{p}^k,\hat{\theta}^k,\hat{\lambda}^k)$ (see Table II). There are multiple advantages of the latter representation. Importantly, some open-system interactions (e.g., the dephasing model explained in detail in Sec. IV) take simpler forms in terms of $(\hat{x}^k,\hat{p}^k,\hat{\theta}^k,\hat{\lambda}^k)$. The momentum and coordinate grids in $(\hat{\boldsymbol{x}}^k,\hat{\boldsymbol{x}}^{k\prime},\hat{\boldsymbol{p}}^k,\hat{\boldsymbol{p}}^{k\prime})$ are interdependent such that if the discretization step size $\boldsymbol{dx}$ and the grid amplitude of $\boldsymbol{x}$ are specified, then the momentum increment $\boldsymbol{dp}$ and the amplitude of $\boldsymbol{p}$ are fixed and vice versa. However, the momentum and position grids in $(\hat{x}^k,\hat{p}^k,\hat{\theta}^k,\hat{\lambda}^k)$ are independent, thus allowing the flexibility to choose dx, dp, and amplitudes of x and p, in order to resolve the quantum dynamics of interest.

The following equation of motion is obtained from Eq. (20):

$$\begin{aligned} i\hbar\frac{d}{dt}|Q\rangle = {}& \overrightarrow{K}\left(\hat{p}_k + \frac{\hbar}{2}\hat{\lambda}_k\right)|Q\rangle - |Q\rangle\overleftarrow{K}\left(\hat{p}_k - \frac{\hbar}{2}\hat{\lambda}_k\right) \\ & + \overrightarrow{V}\left(\hat{x}_k + \frac{\hbar}{2}\hat{\theta}_k\right)|Q\rangle - |Q\rangle\overleftarrow{V}\left(\hat{x}_k - \frac{\hbar}{2}\hat{\theta}_k\right). \end{aligned} \tag{69}$$

The first-order splitting leads to the two-step propagation

$$|Q^{1/2}\rangle = e^{-\frac{idt}{\hbar}\overrightarrow{K}(\hat{p}+\frac{\hbar}{2}\hat{\lambda})}|Q_t\rangle e^{\frac{idt}{\hbar}\overleftarrow{K}(\hat{p}-\frac{\hbar}{2}\hat{\lambda})}, \tag{70}$$

$$|Q_{t+dt}\rangle = e^{-\frac{idt}{\hbar}\overrightarrow{V}(\hat{x}-\frac{\hbar}{2}\hat{\theta})}|Q^{1/2}\rangle e^{\frac{idt}{\hbar}\overleftarrow{V}(\hat{x}+\frac{\hbar}{2}\hat{\theta})}. \tag{71}$$

The employment of the appropriate basis at each step removes the need for arrows:

$$\langle\lambda p|Q^{1/2}\rangle = e^{-\frac{idt}{\hbar}K(p+\frac{\hbar}{2}\lambda)}\langle\lambda p|Q_t\rangle e^{\frac{idt}{\hbar}K(p-\frac{\hbar}{2}\lambda)}, \tag{72}$$

$$\langle x\theta|Q^{1/2}\rangle = \mathcal{F}^{\lambda p\to x\theta}\langle\lambda p|Q^{1/2}\rangle, \tag{73}$$

$$\langle x\theta|Q_{t+dt}\rangle = e^{-\frac{idt}{\hbar}V(x-\frac{\hbar}{2}\theta)}\langle x\theta|Q^{1/2}\rangle e^{\frac{idt}{\hbar}V(x+\frac{\hbar}{2}\theta)}, \tag{74}$$

$$\langle\lambda p|Q^{1/2}\rangle = \mathcal{F}_{x\theta\to\lambda p}\langle\lambda p|Q^{1/2}\rangle, \tag{75}$$

where the Fourier transform conforms with Eqs. (39) and (40) according to

$$\mathcal{F}_{x\theta\to\lambda p} \equiv \mathcal{F}_{x\to\lambda}\mathcal{F}_{\theta\to p} = \mathcal{F}_{\theta\to p}\mathcal{F}_{x\to\lambda}, \tag{76}$$

$$\mathcal{F}^{\lambda p\to x\theta} \equiv \mathcal{F}^{\lambda\to x}\mathcal{F}^{p\to\theta} = \mathcal{F}^{p\to\theta}\mathcal{F}^{\lambda\to x}. \tag{77}$$

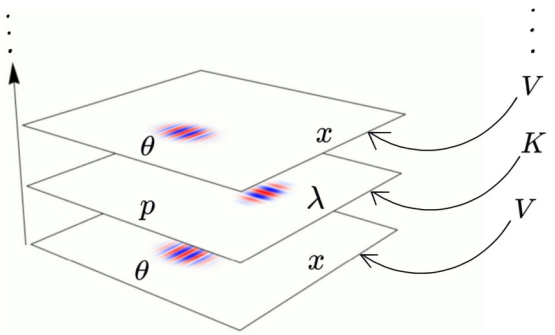

FIG. 4. Schematic representation of the iterative steps to propagate the quantum state according to Eqs. (72)–(75).

A schematic view of the sequence of steps (72)–(75) is shown in Fig. 4. Note that to maintain consistency, the propagator must be solely expressed in terms of contravariant components, e.g.,

$$K\left(p \pm \frac{\hbar}{2}\lambda\right) = c\alpha^k\left(p^k \pm \frac{\hbar}{2}\lambda^k\right) + mc^2\gamma^0/2. \tag{78}$$

The matrix exponentials in Eq. (72) can be evaluated analytically. For instance, assuming a two-dimensional quantum system (ignoring x^3 and p^3) we obtain

$$e^{-\frac{idt}{\hbar}[c\alpha^k p^k + mc^2\gamma^0]} = \begin{pmatrix} \mathcal{K}_{11} & 0 & 0 & \mathcal{K}_{14} \\ 0 & \mathcal{K}_{11} & \mathcal{K}_{23} & 0 \\ 0 & \mathcal{K}_{32} & \mathcal{K}_{11}^* & 0 \\ \mathcal{K}_{41} & 0 & 0 & \mathcal{K}_{11}^* \end{pmatrix}, \tag{79}$$

with

$$\mathcal{K}_{11} = \cos(cdtF/\hbar) - imc\frac{\sin(cdtF/\hbar)}{F}, \tag{80}$$

$$\mathcal{K}_{14} = \frac{\sin(cdtF/\hbar)}{F}(-ip^1 - p^2), \tag{81}$$

$$\mathcal{K}_{23} = -U_{14}^*, \tag{82}$$

$$\mathcal{K}_{32} = U_{14}, \tag{83}$$

$$\mathcal{K}_{41} = -U_{14}^*, \tag{84}$$

$$F = \sqrt{(mc)^2 + (p^1)^2 + (p^2)^2}. \tag{85}$$

Likewise, the exponential in Eq. (74) yields

$$e^{-\frac{idt}{\hbar}[\alpha^\mu eA_\mu + mc^2\gamma^0]} = e^{-\frac{ieA^0dt}{\hbar}}\begin{pmatrix} \mathcal{A}_{11} & 0 & \mathcal{A}_{13} & \mathcal{A}_{14} \\ 0 & \mathcal{A}_{11} & \mathcal{A}_{23} & \mathcal{A}_{24} \\ \mathcal{A}_{31} & \mathcal{A}_{32} & \mathcal{A}_{11}^* & 0 \\ \mathcal{A}_{41} & \mathcal{A}_{42} & 0 & \mathcal{A}_{11}^* \end{pmatrix}, \tag{86}$$

with

$$\mathcal{A}_{11} = \cos(dtG/\hbar) - imc^2\frac{\sin(dtG/\hbar)}{G}, \tag{87}$$

$$\mathcal{A}_{31} = \mathcal{A}_{13} = iA^3\frac{\sin(dtG/\hbar)}{G}, \tag{88}$$

$$\mathcal{A}_{41} = \mathcal{A}_{23} = (-A^2 + iA^1)\frac{\sin(dtG/\hbar)}{G}, \tag{89}$$

$$\mathcal{A}_{32} = \mathcal{A}_{14} = -\mathcal{A}_{41}^*, \tag{90}$$

$$\mathcal{A}_{42} = \mathcal{A}_{24} = \mathcal{A}_{31}^*, \tag{91}$$

$$G = \sqrt{(mc^2)^2 + (A^1)^2 + (A^2)^2 + (A^3)^2}. \tag{92}$$

Having described the propagation for closed-system Dirac evolution, we now proceed to introduce quantum dephasing (46), a particular open-system interaction. According to Eq. (54), the dephasing dynamics enters into the exponential of the potential energy, thereby modifying the propagation step (74) as

$$\langle x\theta|Q_{t+dt}\rangle = e^{-\frac{idt}{\hbar}\tilde{V}(x-\frac{\hbar}{2}\theta)}\langle x\theta|Q^{1/2}\rangle e^{\frac{idt}{\hbar}\tilde{V}(x+\frac{\hbar}{2}\theta)}, \tag{93}$$

with

$$-\frac{idt}{\hbar}\tilde{V}\left(x \pm \frac{\hbar}{2}\theta\right) = -\frac{idt}{\hbar}V\left(x \pm \frac{\hbar}{2}\theta\right) - \frac{Ddt}{2}\theta^2. \tag{94}$$

The replacement of Eq. (74) by Eq. (93) is mathematically equivalent to Gaussian filtering along the momentum axis (i.e., convolution with a Gaussian in momentum) of the coherently propagated $W(t,x^1,p^1)$. This simple interpretation of the dephasing dynamics plays a crucial role in Sec. VI.

The presented algorithm can be implemented with the resources of a typical desktop computer and are well suited for graphics processing units (GPU) computing [116]. In particular, the illustration in the next section was executed with a Nvidia graphics card Tesla C2070.

VI. MAJORANA SPINORS

Hereafter, assuming a one-dimensional dynamics, the Wigner function takes the functional form $W(t,x^1,p^1)$. Furthermore, natural units ($c = \hbar = 1$) are used throughout. In this section, we employ a 512×512 grid for x^1 and p^1 as well as a time step $dt = 0.01$.

Majorana spinors, characterized for being their own antiparticles, are the subject of interest in a broad range of fields including high-energy physics, quantum information theory, and solid state physics [117]. In particular, the solid state counterpart of the relativistic Majorana spinors is known to be robust against perturbations and imperfections due to peculiar topological features [83].

In this section, we study the dynamics of the original Majorana spinor [87] in the presence of dephasing noise (46). Let

$$\psi = \begin{pmatrix} \psi_1 \\ \psi_2 \\ \psi_3 \\ \psi_4 \end{pmatrix} \tag{95}$$

be an arbitrary spinor, then there are two underlying Majorana states (see, e.g., Chap. 12, p. 165, of Ref. [118])

$$\psi_\pm^M = \begin{pmatrix} \psi_1 \\ \psi_2 \\ \psi_3 \\ \psi_4 \end{pmatrix} \pm \begin{pmatrix} -\psi_4^* \\ \psi_3^* \\ \psi_2^* \\ -\psi_1^* \end{pmatrix}. \tag{96}$$

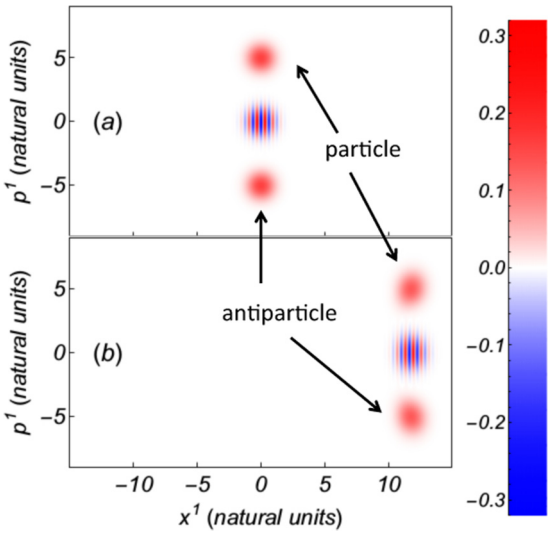

FIG. 5. The relativistic Wigner function $W^0(t,x^1,p^1)$ for a potential-free Majorana spinor ψ_+^M associated with the spinor in Eq. (97) at (a) $t = 0$ and (b) at $t = 12$, upon propagation with Eq. (44). Note that the particle undergoes dephasing with coefficient $D = 0.01$, without an external electromagnetic field. An animated illustration can be found in [119].

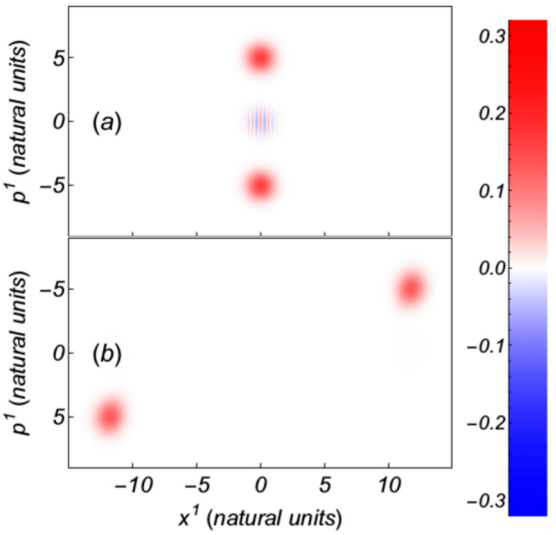

FIG. 6. The relativistic Wigner function $W^0(t,x^1,p^1)$ for a potential-free particle-particle superposition corresponding to the spinor in Eq. (98) at (a) $t = 0$ and (b) at $t = 12$, upon propagation with Eq. (44). Note that the particle undergoes dephasing with coefficient $D = 0.01$, without an external electromagnetic field. An animated illustration can be found in [120].

In particular, we propagate the Majorana spinor ψ_+^M [shown in Fig. 5(a)] obtained from

$$\psi_0 = e^{-\frac{(x^1)^2}{2}+ix^1\tilde{p}^1}(\tilde{p}^0+mc,0,0,\tilde{p}^1)^T, \tag{97}$$

with $\tilde{p}^0 = \sqrt{(\tilde{p}^1)^2+(mc)^2}$ and the numerical values $\tilde{p}^1 = 5$, $m = 1$, and the dephasing coefficient $D = 0.01$ in natural units. The resulting time propagation of ψ_+^M is shown in Fig. 5(b).

Figure 5 reveals that the particle-antiparticle superposition of the Majorana state generates a strong interference in the phase space, which survives an even very intense dephasing interaction. The reason of such robustness is that both the particle component (with a positive momentum) and the antiparticle component (with a negative momentum) move in *parallel* along the positive spatial direction. This is in agreement with the interpretation of antiparticles as particles moving backwards in time. In other words, the velocity and momentum are colinear for particles (see animation [120]) but anticollinear for antiparticles (see animation [119]). The interference fringes, consisting of negative and positive stripes, also remain parallel to the momentum axis (i.e., Majorana spinors carry its interference). Considering the remark after Eq. (93), the action of dephasing is equivalent to the Gaussian filtering along the p^1 axis only. This mixes negative values with negative, positive values with positive, but never positive with negative values of the Wigner function. Hence, this leaves the interference stripes invariant. In other words, free Majorana spinors evolve in a decoherence-free subspace [121] for the bath model in Eq. (46).

The described Majorana state dynamics is fundamentally different from the evolution of a cat state, i.e., a particle-particle superposition. For example, up to a normalization factor, consider the following initial cat state, composed of mostly particles:

$$\psi_0 = e^{-\frac{(x^1)^2}{2}}\left[e^{ix^1\tilde{p}^1}+e^{-ix^1\tilde{p}^1}\right](\tilde{p}^0+mc,0,0,\tilde{p}^1)^T. \tag{98}$$

Figure 6 depicts the evolution of this state under the influence of the same dephasing interaction as in Fig. 5. Contrary to the Majorana case, the negative momentum components of the cat state are made of particles; therefore, we observe in Fig. 6 that they move along the negative spatial direction. The interference stripes connecting the positive (moving to the right) and negative (moving to the left) momentum components no longer remain parallel with respect to the p^1 axis. Thus, dephasing occurs as the Gaussian filtering averages over positive and negative stripes, thereby washing interferences out.

We note that the distortion from the original Gaussian character of particle and antiparticle states at initial time in Figs. 5 and 6 is due to the momentum dispersion.

The total integrated negativity of the Wigner function is

$$N(t) = \int_{W^0(t,x^1,p^1)<0} W^0(t,x^1,p^1)dx^1dp^1. \tag{99}$$

In nonrelativity [58,59], the negativity of the Wigner function is widely regarded as a measurement of the quantum coherence because interferences are associated with negative values. In relativity, there are three physically distinct types of interferences: (i) particle-particle (e.g., the cat state in Fig. 6), (ii) antiparticle-antiparticle, and (iii) particle-antiparticle, that is, *zitterbewegung* (e.g., the Majorana state in Fig. 5). A positive Wigner function is an indicator of classicality in nonrelativity. In relativity, however, there are a broad range of pure states, containing both particles and antiparticles, with underlying positive Wigner functions [57]. This implies that a single snapshot of a relativistic Wigner function does not offer enough information to distinguish particles from antiparticles.

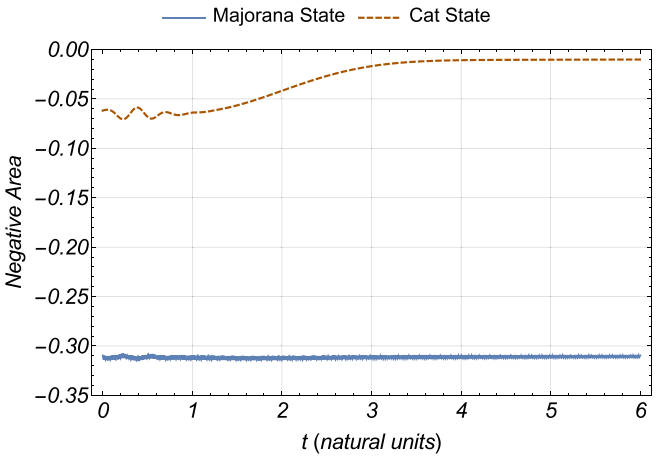

FIG. 7. Negativity (99) of the Majorana state (a particle-antiparticle superposition) in solid line corresponding to the free evolution presented in Fig. 5 in comparison with the negativity of the cat state (a particle-particle superposition) in dashed lines corresponding to Fig. 6.

This difference becomes evident only during time evolution since the momentum direction coincides with the direction of motion for portions of the Wigner function associated with particles, whereas the momentum direction is opposite to the direction of motion for antiparticles.

Figure 7 shows that the negativity of the cat state reduces, while the negativity of the Majorana state is constant.

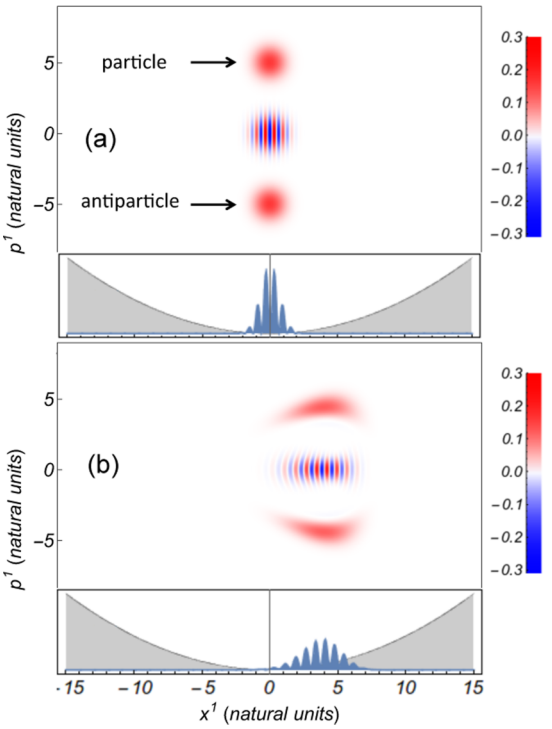

FIG. 8. (a) Initial Majorana state extracted from (97), along with its marginal distribution in position where the gray area represents the underlying mass modulated potential $m \to m + 0.05(x^1)^2$. (b) Propagated Majorana state at time $t = 14$. An animated illustration can be found in [122].

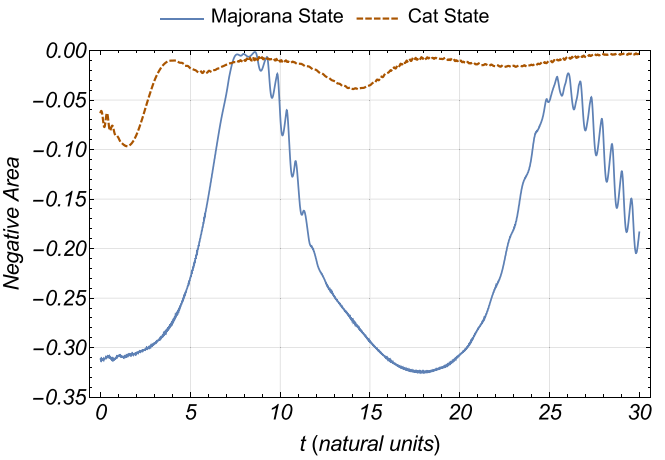

FIG. 9. Negativity of the Majorana state of Fig. 8 in solid line, compared to the negativity of the corresponding cat state.

Moreover, the negativity of the free Majorana spinor remains constant even for extreme values of the decoherences. Therefore, this robustness is not a perturbative effect with respect to the dephasing coefficient D. Note that Majorana spinor's initial negativity is more pronounced than that of the cat state (Fig. 7). Hence, Majorana states are more coherent than cat states.

Having studied free evolution, we now proceed to a Majorana state evolving under the influence of the spatially modulated mass $m \to m + 0.05(x^1)^2$. This type of system also maintains a high coherence despite significant dephasing

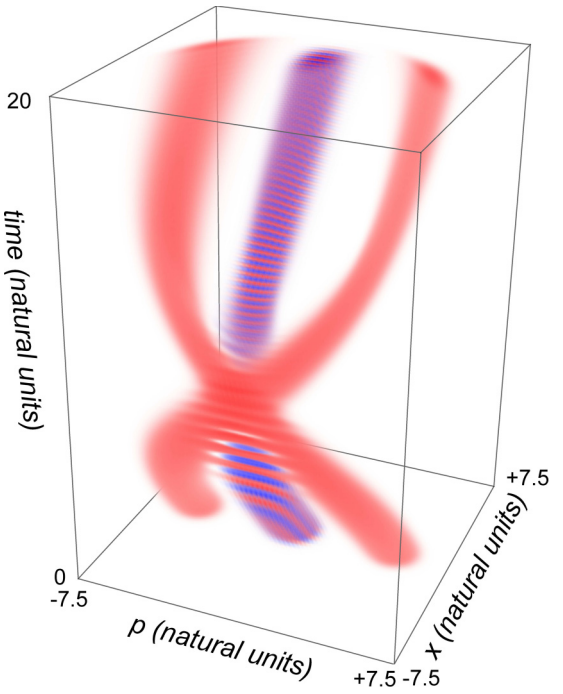

FIG. 10. Time-stacked relativistic Wigner function ($0 \leqslant t \leqslant 20$) for the Majorana dynamics shown in Fig. 8. The interferences, located in the middle, remain robust all along the evolution despite of the presence of significant quantum decoherence. The inteferences contain regions of negative value in blue. The integrated negativity (99) as a function in time is shown in Fig. 9.

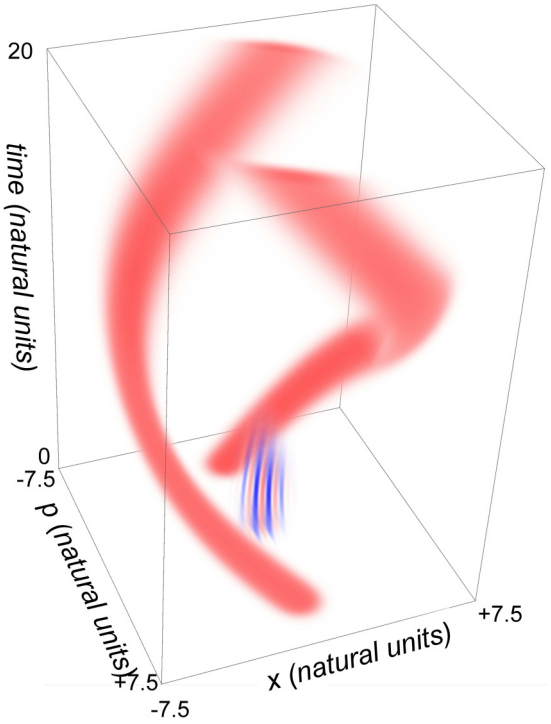

FIG. 11. Time-stacked relativistic Wigner function ($0 \leqslant t \leqslant 20$) for a cat state evolving in the same potential as the Majorana spinor in Fig. 10. The interferences fade shortly after the initiation of the propagation due to the action of quantum decoherence. The integrated negativity (99) as a function in time is shown in Fig. 9.

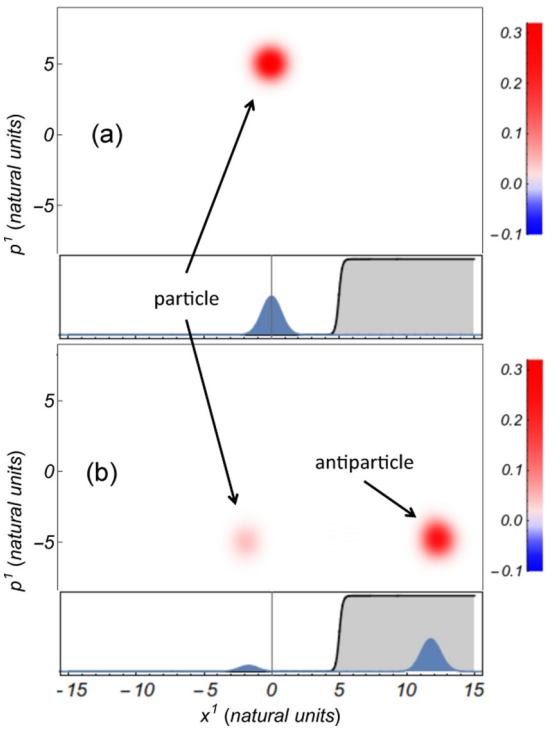

FIG. 12. Illustration of the Klein paradox in terms of the relativistic Wigner function with an underlying decoherence process with coefficient $D = 0.05$. The step potential $A_0 = 10\{1 + \tanh[4(x - 5)]\}/2$ is depicted as a gray area. The height of the step potential is $V_0 = 10$ while the energy of the initial wave packet is $E = 5.01$. (a) The initial state $W^0(t = 0, x^1, p^1)$ from Eq. (97) with $\tilde{p}^1 = 5$ aimed towards the barrier. (b) Final state of the relativistic Wigner function at $t = 12$ made of mostly a negative energy wave packet (antiparticle) being transmitted through the barrier. See the animation in Ref. [125].

$D = 0.01$. The initial Majorana state is shown in Fig. 8(a) while the propagated state at time $t = 14$ is shown in Fig. 8(b). The latter figure shows that interference is preserved. (See the Majorana state animation in Ref. [122] and the corresponding cat state animation in Ref. [123].) A comparison of the negativities for Majorana and cat states as functions of time are shown in Fig. 9, where the Majorana state negativity oscillates albeit with some decay, which is much slower than the cat-state decay. Figure 10, showing the full Wigner dynamics, sheds light on the revival of the Majorana's negativity: when the particle and antiparticle components merge and separate, the negativity disappears and appears, respectively. The corresponding full dynamics of the cat state is shown in Fig 11 displaying a fast disappearance of the interferences.

VII. KLEIN TUNNELING

As the second numerical example, we examine the Klein paradox [124], an unexpected consequence of the Dirac equation, predicting that a positive energy particle colliding with a sharp potential barrier of the height $V > mc^2$ is transmitted as a negative energy state. For example, the initial state (97) with $\tilde{p}^1 = 5, m = 1$ is shown in Fig. 12(a) along with the potential $A_0 = 10\{1 + \tanh[4(x - 5)]\}/2$. We observe in Fig. 12(b) that most of the wave packet has been transmitted as antiparticles. (See animation in Ref. [125].)

An important extension of the Klein paradox is the Klein tunneling, where the step potential is replaced by a finite width barrier. In this case, the theoretical prediction specifies a high transmission even for a wide barrier. Condensed matter analogies of this phenomenon are a subject of active research [7,126]. Three snapshots of the Klein tunneling dynamics are shown in Fig. 13, where (a) corresponds to the positive energy initial state, (b) the state penetrating the potential barrier as antiparticle, and (c) the final state emerging from the barrier as particle. (See animation in Ref. [127].)

The Dirac particle has a spinorial as well as a configurational degree of freedom. The Klein tunneling can be viewed as an interband transition between positive and negative energy states [128]. Analogous effects exist in nonrelativistic dynamics. In particular, compared to the structureless case, nonrelativistic systems with many degrees of freedom manifest many unique peculiarities such as, e.g., transmission rate enhancement [129,130] and directional symmetry breaking [131]. Thus, the energy exchange between different degrees of freedom underlies the counterintuitive dynamics of both the Klein and the nonrelativistic tunneling of particles with internal structure.

Furthermore, the Klein tunneling can be interpreted as the Landau-Zener transition between positive and negative energy states. This conclusion is obtained, e.g., by comparing Eqs. (B8) and (B9) (setting $A^\mu = 0$) with Eqs. (19)–(21) in Ref. [132]. This observation underscores an analogy between solid state and relativistic physics.

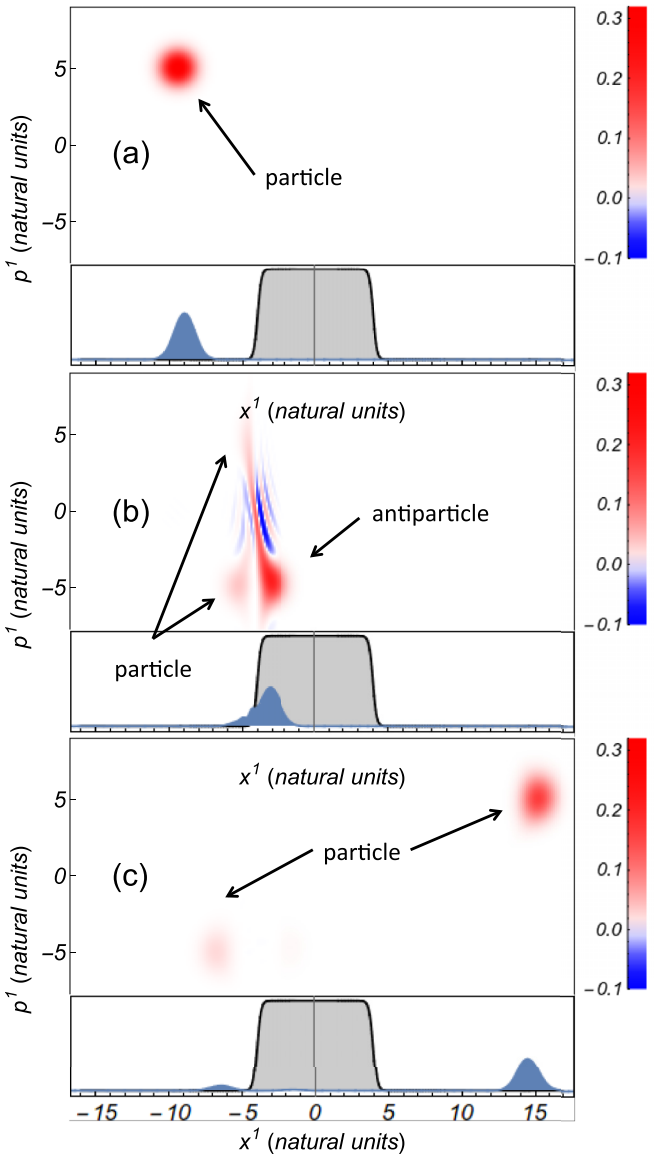

FIG. 13. Illustration of the Klein tunneling in terms of the relativistic Wigner function with the potential barrier $A_0 = 5\{\tanh[4(x+4)] + \tanh[4(-x+4)]\}$ depicted as a gray area. The system undergoes a decoherence process with $D = 0.05$. (a) The relativistic Wigner function $W^0(t=0, x^1, p^1)$ for the initial state in Eq. (97) with $\tilde{p}^1 = 5$ and positioned around $x^1 = -10$. (b) The relativistic Wigner function at $t = 6$ in the process of entering the potential and transforming into a negative energy wave packet (antiparticle). (c) The final relativistic Wigner function at $t = 24$, where most of the initial wave packet has been transmitted as a positive energy wave packet (particle). See the animation in Ref. [127].

Simulations with different values of the dephasing coefficient D have been performed in order to investigate the effect of decoherence on the final transmission. Figure 14 depicts the integrated negativity (99) as a function of time for three different values of D. The evolution without decoherence generates high negativity that indicates interference between the larger transmitted and smaller reflected wave packets. In the same figure we observe that the decoherence eliminates negativity at later stages of the propagation. Nevertheless,

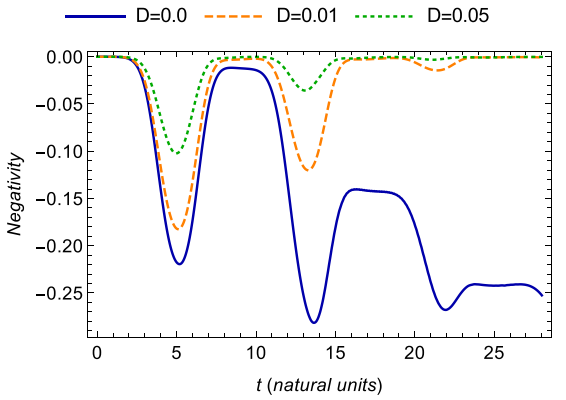

FIG. 14. The integrated negative area in Eq. (99) as a function of time for the Klein tunneling process. Three different values of the decoherence coefficient are considered for the same initial state depicted in Fig. 13(a). The first dip corresponds to the first contact of the wave packet with the barrier as shown in Fig. 13(b). The second dip corresponds to the main wave packet emerging from the barrier. This emerging packet comes along a smaller packet reflected inside the barrier that later generates a third dip when it encounters the left side of the barrier. This process continues generating smaller and smaller dips for packets moving inside the barrier.

the effect of decoherence on the final transmission rate is small in Fig. 15, where the transmission as a function of time nearly coincides for different values of D. We also note a weak dependence of the antiparticle generation on the dephasing coefficient as shown in Fig. 16. Contrary to nonrelativistic quantum dynamics [24,25,28–30,32,41,95], decoherence in the relativistic regime does not recover a single-particle classical description. Furthermore, we show in Appendix B that *the limit* $\hbar \to 0$ *of the Dirac equation leads to two classical Hamiltonians*: one describing particles with a forward advancing clock (i.e., particles), while the other a particle with backward flowing proper time (i.e., antiparticles). (This limit of the Dirac equation represents an

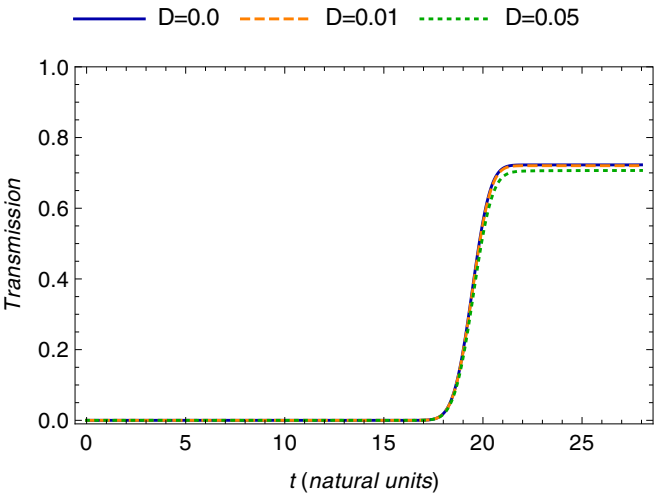

FIG. 15. The Klein transmission across the potential barrier as a function of time for the initial wave packet shown in Fig. 13(a), indicating a weak dependence on the dephasing intensity.

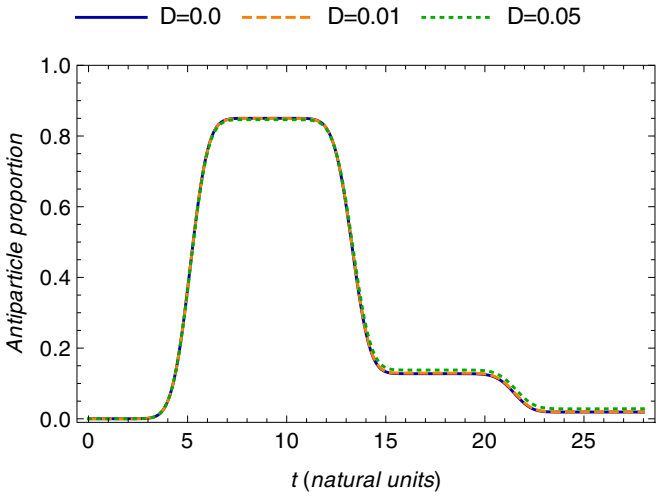

FIG. 16. The antiparticle proportion as a function of time for three different values of the decoherence coefficient in the Klein tunneling process. The initial state composed of mostly particles is shown in Fig. 13(a). The first high plateau corresponds to the period of time when most of the wave packet travels within the potential barrier as an antiparticle. Once this wave packet emerges out of the barrier, there is a smaller reflected packet that moves to the left inside the barrier yielding the second plateau.

example of classical Nambu dynamics [133].) This explains the persistence of positive energy states even for strong dephasing. We believe that the latter observation should also hold in condensed matter physics.

VIII. CONCLUSIONS

We introduced the density matrix formalism for relativistic quantum mechanics as a generalization of the spinorial description of the Dirac equation. This formalism is employed to describe interactions with an environment. Moreover, we presented concise and effective numerical algorithms for the density matrix as well as the relativistic Wigner function propagation.

As a particularly important case, a Lindbland model of quantum dephasing was studied. While decoherence eliminated interferences, the particular structure of a free Majorana spinor remained robust. Partial robustness was also observed for a coordinate-dependent mass term in the Dirac equation. This robustness represents yet another remarkable attribute of Majorana spinors [134] not presently acknowledged, which may be important experimentally. Moreover, the dynamics of the Klein paradox as well as Klein tunneling turned out to be weakly affected by quantum dephasing.

The presented numerical approach opens new horizons in a number of fields such as relativistic quantum chaos [135], the quantum-to-classical transition, and experimentally inspired relativistic atomic and molecular physics [136–138]. Additionally, our method can be used to simulate effective systems modeled by relativistic mechanics, e.g., graphene [139,140], trapped ions [14], optical lattices [141], and semiconductors [142,143]. Finally, the developed techniques can be generalized to treat Abelian [51,144,145] as well as non-Abelian [2,146] (e.g., quark gluon) plasmas.

ACKNOWLEDGMENTS

The authors thank W. Zurek for insightful comments. R.C. is supported by Grant No. DOE DE-FG02-02ER15344, D.I.B. and H.A.R. are partially supported by Grant No. ARO-MURI W911NF-11-1-0268. A.C. acknowledges the support of the Fulbright Program. D.I.B. was also supported by 2016 AFOSR Young Investigator Research Program.

APPENDIX A: LORENTZ COVARIANCE OF THE DIRAC EQUATION

A vector in Feynman's slash notation reads as

$$\not{u} = u^\mu \gamma_\mu, \tag{A1}$$

where the gamma matrices obey the following Clifford algebra:

$$\gamma_\mu \gamma_\nu + \gamma_\nu \gamma_\mu = 2 g_{\mu\nu} \mathbf{1}, \tag{A2}$$

with $g_{\mu\nu} = \mathrm{diag}(1,-1,-1,-1)$. The restricted Lorentz transform does not carry out reflections and preserves the direction of time and belongs to the group referred as $SO_+(1,3)$. In the present case, the transformation for the vector $\not{u}$ is carried out in terms of Lorentz spinors L belonging to the double cover group of $SO_+(1,3)$, according to

$$\not{u} \to \not{u}' = L \not{u} L^{-1}. \tag{A3}$$

The concept of a spinor as an operator can be found, for example, in Chap. 10 of Ref. [118]. The double cover of $SO_+(1,3)$ is known as the $\mathbf{Spin}_+(1,3)$ group and is precisely defined as

$$\mathbf{Spin}_+(1,3) = \{L \in \mathrm{Matrices}(4,\mathbb{C}) |\, L\gamma^0 L^\dagger \gamma^0 = \mathbf{1}\}. \tag{A4}$$

For this type of Lorentz transform the inverse can be obtained as [118]

$$L^{-1} = \gamma^0 L^\dagger \gamma^0. \tag{A5}$$

The restricted Lorentz transform can also be carried out by the action of the complex special linear group $SL(2,\mathbb{C}) \simeq \mathbf{Spin}_+(1,3)$ [118,147,148], which is made of 2×2 complex matrices with determinant one. The proper orthochronous Lorentz transformations can be parametrized by six variables denoting rotations and boots

$$L = \exp\left(\tfrac{1}{2}\eta_k \gamma^0 \gamma^k\right) \exp\left(\tfrac{1}{4}\epsilon_{jkl}\theta^j \gamma^k \gamma^l\right), \tag{A6}$$

where θ^j represent three rotation angles, η_k three boosts (rapidity variables), and $\gamma^\mu = \gamma_\mu^{-1}$. The proper velocity can be obtained as the active boost of the proper velocity of a particle initially at rest with proper velocity $\not{u}_{\mathrm{rest}} = \gamma^0$. This means that in general it is possible to find a Lorentz spinor L such that

$$\not{u} = L \not{u}_{\mathrm{rest}} L^{-1} = L L^\dagger \gamma^0. \tag{A7}$$

This expression indicates that the information stored in the 4-vector $\not{u}$ can be carried out by the associated Lorentz rotor L and the fixed reference 4-vector $\not{u}_{\mathrm{rest}}$.

The Lorentz transformation in Eq. (A3) implies that

$$\bar{u}_\mu \gamma^\mu = L u_\mu \gamma^\mu L^{-1}. \tag{A8}$$

Considering that u_μ transforms as the components of a covariant tensor, we obtain

$$u_\nu \frac{\partial x^\nu}{\partial x'^\mu}\gamma^\mu = u_\nu L\gamma^\nu L^{-1}, \tag{A9}$$

which implies that

$$L\gamma^\nu L^{-1} = \frac{\partial x^\nu}{\partial x'^\mu}\gamma^\mu. \tag{A10}$$

The Lorentz transformation of a vector field that depends on the space-time position x is carried out in a similar manner as (A3):

$$A(x) \to \bar{A}(\bar{x}) = LA(x)L^{-1}. \tag{A11}$$

Moreover, assuming that the origins of the reference frames coincide,

$$\bar{A}(\bar{x}) = LA(L^{-1}\bar{x}L)L^{-1}. \tag{A12}$$

The Lorentz transformation of a spinorial field is consistent accordingly

$$\psi(x) \to \bar{\psi}(\bar{x}) = L\psi(x) \tag{A13}$$

The manifestly covariant Dirac equation is

$$ic\hbar\gamma^\mu \frac{\partial}{\partial x^\mu}\psi(x) - \gamma^\mu eA_\mu(x)\psi(x) - mc^2\psi(x) = 0, \tag{A14}$$

such that applying the Lorentz rotor L on the left we obtain

$$ic\hbar L\gamma^\mu \frac{\partial}{\partial x^\mu}L^{-1}L\psi(x) - L\gamma^\mu eA_\mu(x)L^{-1}L\psi(x) - mc^2L\psi(x) = 0. \tag{A15}$$

Employing Eq. (A10), the first term of this equation can be written as

$$i\hbar L\gamma^\mu \frac{\partial}{\partial x^\mu}L^{-1}L\psi(x) = i\hbar\frac{\partial x^\mu}{\partial \bar{x}^\nu}\gamma^\nu \frac{\partial}{\partial x^\mu}\bar{\psi}(\bar{x}) \tag{A16}$$

$$= i\hbar\gamma^\nu \frac{\partial}{\partial \bar{x}^\nu}\bar{\psi}(\bar{x}). \tag{A17}$$

Therefore, maintaining the form for the Dirac equation and demonstrating its relativistic covariance

$$i\hbar\gamma^\mu \frac{\partial}{\partial \bar{x}^\mu}\bar{\psi}(\bar{x}) - \gamma^\mu e\bar{A}_\mu(\bar{x})\bar{\psi}(\bar{x}) = mc\bar{\psi}(\bar{x}). \tag{A18}$$

Furthermore, it follows that the relativistic density matrix $P(x,x') = \psi(x)\psi^\dagger(x')\gamma^0$ transforms as

$$P(x,x') \to \bar{P}(\bar{x},\bar{x}') = \bar{\psi}(\bar{x})\bar{\psi}^\dagger(\bar{x}')\gamma^0 \tag{A19}$$

$$= L\psi(x)\psi^\dagger(x')L^\dagger\gamma^0 \tag{A20}$$

$$= L\psi(x)\psi^\dagger(x')\gamma^0\gamma^0L^\dagger\gamma^0 \tag{A21}$$

$$= LP(x,x')L^{-1}. \tag{A22}$$

APPENDIX B: CLASSICAL LIMIT OF THE DIRAC EQUATION

The Dirac equation reads as

$$D\psi = [\gamma^0\gamma^\mu(c\hat{\boldsymbol{p}}_\mu - eA_\mu(\hat{\boldsymbol{x}})) - \gamma^0mc^2]\psi = 0. \tag{B1}$$

In the classical limit, we understand the situation when the operators of the momenta $\hat{p}_\mu$ and coordinates $\hat{x}^\mu$ commute [45,149,150]. Following the Hilbert phase-space formalism [45,94], we separate the commutative and noncommutative parts of the Dirac generator D by introducing the algebra of classical observables

$$[\hat{x}^\mu,\hat{p}_\nu] = 0, \quad [\hat{p}_\mu,\hat{\theta}^\nu] = -i\delta^\nu_\mu, \tag{B2}$$

$$[\hat{x}^\mu,\hat{\lambda}_\nu] = -i\delta^\mu_\nu, \quad [\hat{\lambda}_\mu,\hat{\theta}^\nu] = 0, \tag{B3}$$

which is connected with the quantum observables as

$$\hat{\boldsymbol{x}}^\mu = \hat{x}^\mu - \hbar\hat{\theta}^\mu/2, \quad \hat{\boldsymbol{p}}_\mu = \hat{p}_\mu + \hbar\hat{\lambda}_\mu/2. \tag{B4}$$

Substituting Eq. (B4) into Eq. (B1) and keeping the terms up to the zeroth order in $\hbar$, we get a function of $\hat{x}^\mu$ and $\hat{p}_\mu$. Considering that $\hat{x}^\mu$ and $\hat{p}_\mu$ commute, we drop the hat hereafter such that

$$D = \gamma^0\gamma^\mu(cp_\mu - eA_\mu) - \gamma^0mc^2 + O(\hbar). \tag{B5}$$

Utilizing the following unitary operator U,

$$U = \sqrt{\frac{E_p + mc^2}{2E_p}}\left[\mathbf{1} - \frac{\gamma^k(cp_k - eA_k)}{E_p + mc^2}\right], \tag{B6}$$

$$E_p = \sqrt{(mc^2)^2 + (cp - eA)^k(cp - eA)^k}, \tag{B7}$$

we finally obtain

$$\lim_{\hbar\to 0} UDU^\dagger = \begin{pmatrix} H_+ & & & 0 \\ & H_+ & & \\ & & H_- & \\ 0 & & & H_- \end{pmatrix}, \tag{B8}$$

with

$$H_\pm = cp_0 - eA_0 \pm E_p. \tag{B9}$$

According to Eq. (B9), the Dirac generator D in the classical limit corresponds to a decoupled pair of classical time-extended Hamiltonians. The Hamiltonian H_+ describes the dynamics of a classical relativistic particle, while H_- governs the dynamics of a particle traveling backwards in time, which resembles an antiparticle. These conclusions confirm the results of numerical simulations in the main text, where a Dirac particle was coupled to a bath causing decoherence that physically realizes the $\hbar \to 0$ limit.

[1] W. Greiner, *Relativistic Quantum Mechanics*, Vol. 3 (Springer, Berlin, 1990).

[2] H. Elze, M. Gyulassy, and D. Vasak, Phys. Lett. B **177**, 402 (1986).

[3] R. Hakim, *Introduction to Relativistic Statistical Mechanics* (World Scientific, Singapore, 2011).

[4] A. Zee, *Quantum Field Theory in a Nutshell* (Princeton University Press, Princeton, NJ, 2010).

[5] A. Di Piazza, C. Müller, K. Z. Hatsagortsyan, and C. H. Keitel, Rev. Mod. Phys. **84**, 1177 (2012).
[6] K. Novoselov, A. K. Geim, S. Morozov, D. Jiang, M. Katsnelson, I. Grigorieva, S. Dubonos, and A. Firsov, Nature (London) **438**, 197 (2005).
[7] M. Katsnelson, K. Novoselov, and A. Geim, Nat. Phys. **2**, 620 (2006).
[8] M. Z. Hasan and C. L. Kane, Rev. Mod. Phys. **82**, 3045 (2010).
[9] Q. Zhang and J. Gong, Phys. Rev. A **93**, 032117 (2016).
[10] J. Otterbach, R. G. Unanyan, and M. Fleischhauer, Phys. Rev. Lett. **102**, 063602 (2009).
[11] S. Ahrens, S.-Y. Zhu, J. Jiang, and Y. Sun, New J. Phys. **17**, 113021 (2015).
[12] J. Y. Vaishnav and C. W. Clark, Phys. Rev. Lett. **100**, 153002 (2008).
[13] O. Boada, A. Celi, J. Latorre, and M. Lewenstein, New J. Phys. **13**, 035002 (2011).
[14] R. Gerritsma, G. Kirchmair, F. Zähringer, E. Solano, R. Blatt, and C. Roos, Nature (London) **463**, 68 (2010).
[15] R. Blatt and C. Roos, Nat. Phys. **8**, 277 (2012).
[16] J. Pedernales, R. Di Candia, D. Ballester, and E. Solano, New J. Phys. **15**, 055008 (2013).
[17] W. Liu, Phys. Chem. Chem. Phys. **14**, 35 (2012).
[18] J. Autschbach, J. Chem. Phys. **136**, 150902 (2012).
[19] R. Nandkishore, D. A. Huse, and S. L. Sondhi, Phys. Rev. B **89**, 245110 (2014).
[20] C. Gardiner and P. Zoller, *Quantum Noise*, Vol. 56 (Springer, Berlin, 2004).
[21] F. Petruccione and H.-P. Breuer, *The Theory of Open Quantum Systems* (Oxford University Press, Oxford, 2002).
[22] M. S. Sarandy and D. A. Lidar, Phys. Rev. Lett. **95**, 250503 (2005).
[23] L. Viola, E. Knill, and S. Lloyd, Phys. Rev. Lett. **82**, 2417 (1999).
[24] W. H. Zurek, Rev. Mod. Phys. **75**, 715 (2003).
[25] W. H. Zurek, Phys. Today **44**(10), 36 (1991).
[26] S. L. Adler and A. Bassi, J. Phys. A: Math. Gen. **40**, 15083 (2007).
[27] Z. P. Karkuszewski, C. Jarzynski, and W. H. Zurek, Phys. Rev. Lett. **89**, 170405 (2002).
[28] W. H. Zurek, Phys. Scripta **T76**, 186 (1998).
[29] S. Habib, K. Jacobs, H. Mabuchi, R. Ryne, K. Shizume, and B. Sundaram, Phys. Rev. Lett. **88**, 040402 (2002).
[30] S. Habib, K. Jacobs, and K. Shizume, Phys. Rev. Lett. **96**, 010403 (2006).
[31] M. V. Berry, *Quantum Mechanics: Scientific Perspectives on Divine Action* (Vatican Observatory CTNS Publications, 2001), pp. 41–54.
[32] T. Bhattacharya, S. Habib, and K. Jacobs, Phys. Rev. A **67**, 042103 (2003).
[33] K. Jacobs and D. A. Steck, Contemp. Phys. **47**, 279 (2006).
[34] W. H. Zurek, Nat. Phys. **5**, 181 (2009).
[35] W. Zurek, Nature (London) **412**, 712 (2001).
[36] I. V. Bazarov, Phys. Rev. Spec. Top.–Accel. Beams **15**, 050703 (2012).
[37] A. Gasbarro and I. Bazarov, J. Synch. Radiat. **21**, 289 (2014).
[38] T. Tanaka, Phys. Rev. Spec. Top.–Accel. Beams **17**, 060702 (2014).
[39] D. Blokhintsev, *The Philosophy of Quantum Mechanics* (Springer, Berlin, 2010).
[40] E. J. Heller, J. Chem. Phys. **65**, 1289 (1976).
[41] S. Habib, K. Shizume, and W. H. Zurek, Phys. Rev. Lett. **80**, 4361 (1998).
[42] A. Bolivar, *Quantum-classical Correspondence* (Springer, Berlin, 2004).
[43] C. Zachos, D. Fairlie, and T. Curtright, *Quantum Mechanics in Phase Space: An Overview with Selected Papers* (World Scientific, Singapore, 2005).
[44] R. Kapral, Annu. Rev. Phys. Chem. **57**, 129 (2006).
[45] D. I. Bondar, R. Cabrera, R. R. Lompay, M. Y. Ivanov, and H. A. Rabitz, Phys. Rev. Lett. **109**, 190403 (2012).
[46] A. Polkovnikov, Ann. Phys. (NY) **325**, 1790 (2010).
[47] E. Wigner, Phys. Rev. **40**, 749 (1932).
[48] T. Curtright, D. B. Fairlie, and C. K. Zachos, *A Concise Treatise on Quantum Mechanics in Phase Space* (World Scientific, Singapore, 2013).
[49] R. Hakim and J. Heyvaerts, Phys. Rev. A **18**, 1250 (1978).
[50] R. Hakim and H. Sivak, Ann. Phys. (NY) **139**, 230 (1982).
[51] D. Vasak, M. Gyulassy, and H. Elze, Ann. Phys. (NY) **173**, 462 (1987).
[52] Y. Yuan, K. Li, J. Wang, and K. Ma, Int. J. Theor. Phys. **49**, 1993 (2010).
[53] M. Kai, W. Jian-Hua, and Y. Yi, Chin. Phys. C **35**, 11 (2011).
[54] S. Varró and J. Javanainen, J. Opt. B: Quantum Semiclassical Opt. **5**, S402 (2003).
[55] A. Larkin and V. Filinov, Phys. Lett. A **378**, 1876 (2014).
[56] K. Kowalski and J. Rembieliński, Ann. Phys. **375**, 1 (2016).
[57] A. G. Campos, R. Cabrera, D. I. Bondar, and H. A. Rabitz, Phys. Rev. A **90**, 034102 (2014).
[58] R. Hudson, Rep. Math. Phys. **6**, 249 (1974).
[59] V. Veitch, N. Wiebe, C. Ferrie, and J. Emerson, New J. Phys. **15**, 113037 (2013).
[60] A. Mari and J. Eisert, Phys. Rev. Lett. **109**, 230503 (2012).
[61] I. Bialynicki-Birula, Acta Phys. Austriaca **151**, 111 (1977).
[62] G. R. Shin and J. Rafelski, Phys. Rev. A **48**, 1869 (1993).
[63] H. Spohn, Ann. Phys. **282**, 420 (2000).
[64] J. Bolte and R. Glaser, J. Phys. A **37**, 6359 (2004).
[65] A. Bolivar, J. Math. Phys. **42**, 4020 (2001).
[66] I. Bialynicki-Birula, P. Górnicki, and J. Rafelski, Phys. Rev. D **44**, 1825 (1991).
[67] G. R. Shin, I. Bialynicki-Birula, and J. Rafelski, Phys. Rev. A **46**, 645 (1992).
[68] I. Bialynicki-Birula, EPJ Web Conf. **78**, 01001 (2014).
[69] F. Hebenstreit, A. Ilderton, M. Marklund, and J. Zamanian, Phys. Rev. D **83**, 065007 (2011).
[70] D. Berényi, S. Varró, P. Lévai, and V. V. Skokov, EPJ Web Conf. **78**, 03001 (2014).
[71] A. Blinne and E. Strobel, Phys. Rev. D **93**, 025014 (2016).
[72] D. Kohen, C. Marston, and D. Tannor, J. Chem. Phys. **107**, 5236 (1997).
[73] D. I. Bondar, R. Cabrera, A. Campos, S. Mukamel, and H. A. Rabitz, J. Phys. Chem. Lett. **7**, 1632 (2016).
[74] A. G. Campos, R. Cabrera, D. I. Bondar, and H. A. Rabitz, arXiv:1502.03025.
[75] B. A. Bernevig and T. L. Hughes, *Topological Insulators and Topological Superconductors* (Princeton University Press, Princeton, NJ, 2013).
[76] Z. Wang, A. Alexandradinata, R. J. Cava, and B. A. Bernevig, Nature (London) **532**, 189 (2016).

[77] B. Lv, H. Weng, B. Fu, X. Wang, H. Miao, J. Ma, P. Richard, X. Huang, L. Zhao, G. Chen *et al.*, Phys. Rev. X **5**, 031013 (2015).

[78] H. Inoue, A. Gyenis, Z. Wang, J. Li, S. W. Oh, S. Jiang, N. Ni, B. A. Bernevig, and A. Yazdani, Science **351**, 1184 (2016).

[79] J. Alicea, Rep. Prog. Phys. **75**, 076501 (2012).

[80] A. Bühler, N. Lang, C. V. Kraus, G. Möller, S. D. Huber, and H. P. Büchler, Nat. Commun. **5**, 4504 (2014).

[81] S. Nadj-Perge, I. K. Drozdov, J. Li, H. Chen, S. Jeon, J. Seo, A. H. MacDonald, B. A. Bernevig, and A. Yazdani, Science **346**, 602 (2014).

[82] C. Nayak, S. H. Simon, A. Stern, M. Freedman, and S. Das Sarma, Rev. Mod. Phys. **80**, 1083 (2008).

[83] S. Albrecht, A. Higginbotham, M. Madsen, F. Kuemmeth, T. Jespersen, J. Nygård, P. Krogstrup, and C. Marcus, Nature (London) **531**, 206 (2016).

[84] S. Diehl, E. Rico, M. A. Baranov, and P. Zoller, Nat. Phys. **7**, 971 (2011).

[85] J. C. Budich, S. Walter, and B. Trauzettel, Phys. Rev. B **85**, 121405 (2012).

[86] J. R. Wootton, J. Burri, S. Iblisdir, and D. Loss, Phys. Rev. X **4**, 011051 (2014).

[87] E. Majorana, Nuovo Cimento **14**, 171 (1937).

[88] T. A. Welton, Phys. Rev. **74**, 1157 (1948).

[89] W. E. Baylis and J. Huschilt, Phys. Lett. A **301**, 7 (2002).

[90] A. Ilderton and G. Torgrimsson, Phys. Rev. D **88**, 025021 (2013).

[91] J. Eisert, M. Friesdorf, and C. Gogolin, Nat. Phys. **11**, 124 (2015).

[92] R. D. Sorkin, arXiv:gr-qc/9507057.

[93] H.-P. Breuer and F. Petruccione, *Relativistic Quantum Measurement and Decoherence: Lectures of a Workshop Held at the Istituto Italiano per gli Studi Filosofici Naples, April 9-10, 1999*, Vol. 559 (Springer, Berlin, 2000).

[94] D. I. Bondar, R. Cabrera, D. V. Zhdanov, and H. A. Rabitz, Phys. Rev. A **88**, 052108 (2013).

[95] R. Cabrera, D. I. Bondar, K. Jacobs, and H. A. Rabitz, Phys. Rev. A **92**, 042122 (2015).

[96] M. Alcubierre, *Introduction to 3 + 1 Numerical Relativity*, Vol. 140 (Oxford University Press, Oxford, New York, 2008).

[97] F. Bopp, Ann. Inst. H. Poincare **15**, 81 (1956).

[98] M. Hillery, M. Scully, E. Wigner *et al.*, Phys, Rep. **106**, 121 (1984).

[99] M. A. Man'ko and V. I. Man'ko, Phys. Scripta **T147**, 014020 (2012).

[100] A. B. Migdal, Phys. Rev. **103**, 1811 (1956).

[101] D. I. Blokhintsev, J. Phys. U.S.S.R. **2**, 71 (1940).

[102] D. I. Blokhintsev and P. Nemirovsky, J. Phys. U.S.S.R. **3**, 191 (1940).

[103] D. I. Blokhintsev and Ya. B. Dadyshevsky, Zh. Eksp. Teor. Fiz. **11**, 222 (1941).

[104] A. Migdal, Dokl. Akad. Nauk SSSR **105**, 77 (1955), see also Ref. [100].

[105] A. Caldeira and A. Leggett, Physica A (Amsterdam) **121**, 587 (1983).

[106] A. C. Doherty and K. Jacobs, Phys. Rev. A **60**, 2700 (1999).

[107] J. Dunkela and P. Hänggi, Phys. Rep. **471**, 1 (2009).

[108] B. Thaller, *The Dirac Equation*, Texts and Monographs in Physics (Springer, Berlin, 1992).

[109] G. R. Mocken and C. H. Keitel, Comput. Phys. Commun. **178**, 868 (2008).

[110] H. Bauke, M. Klaiber, E. Yakaboylu, K. Z. Hatsagortsyan, S. Ahrens, C. Müller, and C. H. Keitel, in *SPIE Optics + Optoelectronics* (International Society for Optics and Photonics, Belligham, WA, 2013), pp. 87801Q–87801Q.

[111] F. Fillion-Gourdeau, E. Lorin, and A. D. Bandrauk, Comput. Phys. Commun. **183**, 1403 (2012).

[112] R. Hammer and W. Pötz, Comput. Phys. Commun. **185**, 40 (2014).

[113] R. Hammer, W. Pötz, and A. Arnold, J. Comput. Phys. **265**, 50 (2014).

[114] R. Beerwerth and H. Bauke, Comput. Phys. Commun. **188**, 189 (2015).

[115] M. Schreilechner and W. Pötz, arXiv:1503.02685.

[116] A. Klockner, N. Pinto, Y. Lee, B. Catanzaro, P. Ivanov, and A. Fasih, Parallel Comput. **38**, 157 (2012).

[117] F. Wilczek, Nat. Phys. **5**, 614 (2009).

[118] P. Lounesto, *Clifford Algebras and Spinors*, Vol. 286 (Cambridge University Press, Cambridge, 2001).

[119] Free majorana evolution, https://youtu.be/2uyGMqHQwOE

[120] Free cat state evolution, https://youtu.be/DvUQgVxdUlo

[121] D. A. Lidar, I. L. Chuang, and K. B. Whaley, Phys. Rev. Lett. **81**, 2594 (1998).

[122] Majorana state propagated in a mass potential, https://youtu.be/hhQWn-GKZO4

[123] Cat state state propagated in a mass potential, https://youtu.be/f3lqxI2wVms

[124] W. Greiner, *Relativistic Quantum Mechanics: Wave Equations* (Springer, Berlin, 2000).

[125] Klein paradox, https://youtu.be/Dvso7GCUm6Y

[126] A. F. Young and P. Kim, Nat. Phys. **5**, 222 (2009).

[127] Klein tunneling, https://youtu.be/gY0xpo-C02M

[128] P. E. Allain and J. Fuchs, Eur. Phys. J. **83**, 301 (2011).

[129] B. Zakhariev and S. Sokolov, Ann. Phys. (NY) **469**, 229 (1964).

[130] D. I. Bondar, W.-K. Liu, and M. Y. Ivanov, Phys. Rev. A **82**, 052112 (2010).

[131] I. Amirkhanov and B. N. Zakhariev, ZhETF **49**, 1097 (1966) [Sov. Phys.–JETP **22**, 764 (1966)].

[132] E. Kane, J. Phys. Chem. Solids **12**, 181 (1960).

[133] Y. Nambu, Phys. Rev. D **7**, 2405 (1973).

[134] S. R. Elliott and M. Franz, Rev. Mod. Phys. **87**, 137 (2015).

[135] R. Tomaschitz, J. Math. Phys. **32**, 2571 (1991).

[136] G. A. Mourou, T. Tajima, and S. V. Bulanov, Rev. Mod. Phys. **78**, 309 (2006).

[137] F. Krausz and M. Ivanov, Rev. Mod. Phys. **81**, 163 (2009).

[138] G. Sarri, W. Schumaker, A. Di Piazza, M. Vargas, B. Dromey, M. E. Dieckmann, V. Chvykov, A. Maksimchuk, V. Yanovsky, Z. H. He *et al.*, Phys. Rev. Lett. **110**, 255002 (2013).

[139] M. Müller, J. Schmalian, and L. Fritz, Phys. Rev. Lett. **103**, 025301 (2009).

[140] O. Morandi and F. Schürrer, J. Phys. A: Math. Theor. **44**, 265301 (2011).

[141] F. Dreisow, M. Heinrich, R. Keil, A. Tünnermann, S. Nolte, S. Longhi, and A. Szameit, Phys. Rev. Lett. **105**, 143902 (2010).

[142] J. Schliemann, D. Loss, and R. M. Westervelt, Phys. Rev. Lett. **94**, 206801 (2005).

[143] W. Zawadzki and T. M. Rusin, J. Phys.: Condens. Matter **23**, 143201 (2011).
[144] J. Mendonça, Phys. Plasmas **18**, 062101 (2011).
[145] F. Haas, B. Eliasson, and P. K. Shukla, Phys. Rev. E **85**, 056411 (2012).
[146] H. Elze and U. Heinz, Phys. Rep. **183**, 81 (1989).
[147] W. E. Baylis, Phys. Rev. A **45**, 4293 (1992).
[148] *Clifford (Geometric) Algebras with Applications to Physics, Mathematics, and Engineering*, edited by W. E. Baylis (Birkhauser, Boston, 1996).
[149] P. Dirac, *The Principles of Quantum Mechanics* (Clarendon, Oxford, 1958).
[150] Yu. M. Shirokov, Fiz. Elem. Chast. At. Yadra **10**, 5 (1979) [Sov. J. Part. Nucl. **10**, 1 (1979)].